Mesoscale Atmospheric Dispersion, 2001, Ed. Z. Boybeyi, WIT Publications, Southampton, UK, Advances in Air Pollution, Vol 9, p. 424.

Chapter 9

Numerical modeling of gas deposition and bi-directional surface–atmosphere exchanges in mesoscale air pollution systems

Devdutta S. Niyogi & Sethu Raman
North Carolina State University
Raleigh, NC 27695–7236, USA
e-mail: dev_niyogi@ncsu.edu
e-mail: sethu_raman@ncsu.edu

Abstract

Accurate representation of surface processes such as vegetation has a significant role in air pollution models. In a variety of situations, the surface acts as a sink for the pollutants. Using pristine relations developed on fluid mechanical concepts, different formulations are discussed in this chapter to develop deposition flux estimates in air pollution models. An interesting scenario also develops when the soil and vegetation, in particular, acts as a source, in addition to being a sink for the gaseous material. Hence as a generalized framework in air pollution systems, the ability of the surface to generate bi-directional fluxes needs to be represented. Accordingly, different modeling techniques are presented ranging from regression equations, to modifications in the resistance pathways, and detailed eco-physiological leaf scaling approach. Finally, of particular relevance to mesoscale applications is the area averaging and regional mapping of the bi-directional fluxes. Accordingly different methods based on combination of surface measurements, remote sensing and model parameterizations are discussed.

Mesoscale Atmospheric Dispersion, 2001, Ed. Z. Boybeyi, WIT Publications, Southampton, UK, Advances in Air Pollution, Vol 9, p. 424.

1 Introduction

One of the important considerations in designing an air pollution modeling system is the accurate and efficient representation of the surface processes. Mathematically, surface processes form a boundary condition in the atmospheric analysis thus becoming a pivotal component of the modeling system for both surface energy balance as well as mass transfer. As discussed in Niyogi and Raman [1], surface processes manifest changes through soil-vegetation-atmosphere-transfer (SVAT) processes in the boundary layer. At the local scale, surface features modulate humidity, temperature, and surface energy balance. At a mesoscale, heterogeneity in surface fluxes leads to mesoscale circulation, which affects transport and diffusion characteristics of the atmosphere. Presence of vegetation thus leads to humidity exchange potential [2]. In addition to its impact on the local as well as regional scale thermodynamic structure, vegetation has a dominant role in air pollution models principally as a sink or a depositing surface [3], [4]. Till mid 1970s most deposition research assumed gases deposit to bare ground with only a marginal impact due to vegetation [5], [6]. Subsequent studies however, have shown that vegetative processes are a dominant pathway for surface–atmosphere exchanges [4], [7], [8], [9], [10].

In this chapter, we will discuss the issues pertaining to mathematically representing surface effects with particular emphasis on pollutant deposition. In the classical sense, such exchange processes have been evaluated principally considering homogeneity. It is being increasingly recognized that one of the largest sources of uncertainty lie in representing surface couplings within the air pollution simulation framework. Though in general, gaseous pollutants are deposited to the surface, in some instances, the vegetation interface can form a source for the biogenic emissions. Hence the biospheric–atmospheric interactions have a dominant role in the atmospheric environmental mass balance, for a variety of applications ranging from regulatory purposes to ecosystem synthesis (see Mooney [11]).

Accordingly, this chapter is structured in the following manner. In the following section, the role of multimedia couplings is discussed both at the micro, and the regional scale. Different gas deposition parameterizations are discussed with particular emphasis on mesoscale

Mesoscale Atmospheric Dispersion, 2001, Ed. Z. Boybeyi, WIT Publications, Southampton, UK, Advances in Air Pollution, Vol 9, p. 424.

models. In Section 3, the land–atmosphere coupling is discussed with particular emphasis on the bi-directional (source as well as sink) exchanges. Here both the modifications in traditional resistance approach as well as more mechanistic plant physiological relations are discussed. One of the pertinent issues for mesoscale models is scaling the parameterizations and the model results to a regional scale. Section 4 therefore outlines the procedures and approaches for regional analysis. Finally, Section 5 presents the conclusions and a discussion for future research in this area.

1.1 Surface processes in environmental analysis

Recent years have witnessed phenomenal growth in the computational resources. Numerical models are being run with higher and higher grid resolution. With increasing horizontal grid resolution, the impact of surface processes becomes increasingly dominant in numerical simulations (see for example, Pielke [12]). Hence, there is a growing concern regarding a realistic representation of the continuum between the surface–atmosphere exchanges [13], [14], [15]. However, most models that consider the coupling between land–air–water, treat the continuum more for energy balance than for mass balance. Hence parameterizations need to be developed for air pollution models and environmental assessment systems in which mass exchange or more correctly gas exchange is explicitly accounted for to provide source/sink representation. We will discuss formulations and development of such parameterizations in this chapter.

In creating a continuum, it is important to develop the coupling by linking the heterogeneous media dynamically. As a general approach, it will be beneficial in developing such couplings so as to integrate different parameterizations and then link it via different conservation equations. Such a system can thus accommodate more than one process and media. This not only allows representation of processes other than linear relations but also provides opportunity for checks and validations of the exchanges. It can also replicate the reality as much as possible in terms of what dominates the pathway and the exchange. Ideally, as discussed earlier, these conservation equations would involve explicit energy as well as mass exchanges. It is important that the system has to be designed with interactive couplings. Also, different processes involved in

Mesoscale Atmospheric Dispersion, 2001, Ed. Z. Boybeyi, WIT Publications, Southampton, UK, Advances in Air Pollution, Vol 9, p. 424.

the coupling should be sensitive to direct as well as second–order or indirect changes and thus show variations for reaction as well as the stimuli. Consequently, the system has to be generalized so as to show valid spatial and temporal variations. Hence the equations that form coupling interfaces in the system need to have prognostic variables and have some form of landscape or regional factors embedded in their specification. Finally the coupled system has to be tested with observations made under different conditions for verification.

Consider an example of a coastal watershed. They are important regions of socio-economic activities for which the environmental issues (air and water quality) have significant implications. The multi-media (land, air water) exchanges form critical pathways for pollutant as well as nutrient transfer. The pollutants released on the land would be either detained on the soil surface, or deposited over the vegetation. This material can subsequently transport through runoff or percolate into the soil and roots and affect the ground water. Portion of the pollutant, which is not detained on the landmasses, is passed over the water body. The terrestrial loading can thus induce changes in the water nutrient status and affect flora and fauna. An additional feature of such a watershed is the mesoscale variability in the surface, subsurface and the meteorological features which can affect the hydro-meteorological exchanges. These features need to be resolved through a mesoscale model with the multimedia systems coupled to it.

1.2 Developing the mathematical framework

In developing the simulation framework the first principle approach can be adopted. As that, pristine laws related to the laminar and turbulent fluid flows are modified to represent the boundary conditions. Typical examples of the extension of such principles are the wind profile 'laws', development of the mixing length (see Holt and Raman [16]), turbulent kinetic energy closure schemes, and the atmospheric boundary layer similarity theories (see Stull [17]). Such fundamental fluid assumptions have been extended in almost every numerical as well as analytical model developed for environmental simulations. The equations and models for simulating the atmospheric or oceanic phenomena have some fundamental assumptions at their core. One such assumption is surface homogeneity. However in recent years, there have been significant

Mesoscale Atmospheric Dispersion, 2001, Ed. Z. Boybeyi, WIT Publications, Southampton, UK, Advances in Air Pollution, Vol 9, p. 424.

improvements in the modeling strategies. More and more realistic features are being incorporated in the model equations, with emphasis on linking causal behavior within heterogeneous systems.

Interfacing heterogeneous media in its simplest form involves development of equations, which pass on the base state at System-1 boundary condition as the initial state for the System-2 boundary. However, this transition is not easy as the two systems cannot be treated in a homogeneous state. There has to be a buffer or interface layer that can act as a moderator for the two boundary conditions to be in congruence with the prevailing environments (without shocking or destabilizing the local equilibrium). This intrinsic concept will be discussed for applications involving water vapor and other gas exchanges and deposition over vegetation (canopy, leaf, stomata and intercellular conduits) and atmospheric boundary.

In the following section, we review some of the underlying principles and assumptions of gas exchange for differential media, including the approximations made in experimental field studies for toxic deposition and exchange. Then, we discuss the techniques, and approaches for vapor exchange at vegetation–atmosphere interface. Finally, we present a discussion summary and conclusions regarding some of the limitations and developments for next generation models.

2 Developing gas deposition relations

Understanding the transport and fate of gaseous pollutants is important for diverse applications. For example, it is now widely recognized plants emit volatile organic compounds (VOCs) such as monoterpene and isoprene (cf. Arey [18]). These biogenic emissions can undergo photolysis and other chemical transformation and generate pollutants such as ozone in the lower troposphere [19]. Results from both special observational campaigns (e.g., Monson and Fall [20]) as well as numerical modeling studies (e.g., Langford and Fehsenfeld [21]; Gunther et al. [22]) confirm this feature at diverse scales. For instance, Fitzgerald [23] estimated that, of the 6000 to 7500 tons of mercury emitted into the atmosphere, 25–50 % is released from natural surfaces.

In addition to being a source of biogenic emission and other primary as well as secondary pollutants, the terrestrial biosphere is known to be a significant sink (see Wesley [24]). The gaseous pollutants can either deposit to the vegetated surface or be absorbed into the leaf cells itself. This exchange between the terrestrial biosphere and the atmosphere thus results in a net reduction of the available pollutant in a mass balance analysis. Hence, the role of the vegetative surfaces both as a source as well as sink is not isolated from each other and is in fact interactive (see Fowler and Unsworth [25], Fuentes and Gillispie [26], and Gao et al. [27]). Such an issue has to be addressed as a continuum problem. The release is therefore from, what can be referred to as, the VOC-rich surface. In the atmosphere, it undergoes transformation as well transport and diffusion in the air medium. Indeed the gases (and the transformed aerosols) subsequently deposit back to the surface. Atmospheric deposition thus plays a pivotal role in determining both the air as well as water and the airshed/watershed quality at a regional scale [28]. The deposited toxin, over land or water, through the continuum impacts regional hydrology, and the air quality both at diurnal as well as climatic scales, depending on its residence time in the ecosystem. Such a scenario, for instance, has been considered to be a major contributor of pollutant recycling in various North American lakes and watersheds [29]. Hence it is critical to introduce the bi-directional role of vegetation and natural surfaces in an environmental analysis.

In order to develop such couplings regarding the source/sink characteristics of natural surfaces, several different approaches have been addressed in the literature. We will review some of the underlying concepts and formulations here.

2.1 Modeling surface deposition flux

For different pollutants including VOCs, the concentration flux can be represented as:

$$F_i = -(D_i + K_i).\, dC/dz, \tag{1}$$

where D_i is the molecular diffusivity, K_i is the respective eddy diffusivity, and dC/dz is the vertical gradient of the concentration. Based on results from several empirical formulations such as Businger [30], and Droppo [31], K_i is taken equal to the eddy diffusivity of heat, K_h. Integrating eqn. (1) assuming a constant flux layer near the surface, yields:

Mesoscale Atmospheric Dispersion, 2001, Ed. Z. Boybeyi, WIT Publications, Southampton, UK, Advances in Air Pollution, Vol 9, p. 424.

$$F_i = - (R_a + R_b)^{-1} (C_r - C_s), \tag{2}$$

where, R_a and R_b are the turbulent aerodynamic and molecular bulk boundary layer resistance for gas exchange, and C_r, C_s are gas concentrations at the reference level (model lowest level) and the surface. The turbulent resistance is the total resistance across the turbulent layer and can be estimated by integrating the changes in the vertical eddy diffusivity for heat between a thickness comprising of ***d*** and z_r, that is the layer above the molecular exchange and the model reference level. Using similarity equations,

$$R_a = Pr .(u_*.k)^{-1}. [\ln (z_r - d)/ (\delta - d) - \Psi_h]. \tag{3a}$$

In the above, in addition to the terms described before, *Pr* is the Prandtl number (0.923 in neutral conditions), u_* is friction velocity, and Y_h is the non-dimensional stability function for heat [32], [33]. Under neutral conditions [34], [35] eqn. (3a) becomes,

$$R_a = Pr. u / u_*^2. \tag{3b}$$

The molecular bulk resistance, on the other hand, is obtained by integrating the total molecular as well as eddy diffusivity between the receptor surface, z_s, and the molecular layer, ***d***. Using similarity relations the boundary layer resistance can be represented as,

$$R_b = (u_*.k)^{-1}. [\ln (z_o/ \delta)]. \tag{4a}$$

Since it is difficult to prescribe or determine the molecular layer thickness, empirical approaches are adopted. A simplification can be adopted for vegetation canopies, yielding [36], $R_b=A.(l/ u)^{0.5}$; where l is the characteristic length scale of the leaf canopy (order of 0.05 m), and A is a constant (~90 $s^{1/2}$ m^{-1}). Similarly, following Owen and Thompson [37], eqn. (4a) can be represented as,

$$R_b = (u_*.B)^{-1}, \tag{4b}$$

where *B* is the interfacial sublayer Stanton number. However, estimations involving *B* are still largely uncertain (see a discussion by Kramm et al. [38]). With increasing turbulence, values of *B* range from 1 to 1.25. Over vegetation canopies, under turbulent conditions, Parlange et al. [39] obtain *B*=2.5, which have been applied in studies such as Leuning et al. [40]. Following theoretical considerations of Owen and Thompson [37],

Mesoscale Atmospheric Dispersion, 2001, Ed. Z. Boybeyi, WIT Publications, Southampton, UK, Advances in Air Pollution, Vol 9, p. 424.

Schlichting [41] and Brutsaert [42] for example, the Stanton number can be estimated as,

$$B^{-1} = a.\ Sc^{b}.\eta^{c}\ . \tag{4c}$$

In the above equation, following Kramm et al. [38], a=0.52, b=0.8, and c=0.45, and h is the roughness Reynolds number. For aerodynamically rough surface, $h=u_{*}.(z_o+d)/n$, while for aerodynamically smooth surface, eddy diffusivity can be solved for the Reynolds number:

$$K_m / \nu = \kappa\,(\eta - 11\tanh(\eta/11))\ . \tag{4d}$$

Another approach for calculating R_b [43], [44],

$$R_b = Pr\,(2 / k.u_{*}).(Sc^{\,0.67})\ , \text{or} \tag{5a}$$

$$R_b = 1.47\ Sc^{0.67}\,(l/uv)^{0.5}\,B^{-1}\ , \tag{5b}$$

where, Sc is the Schmidt number, which is the ratio of the kinematic viscosity and the diffusivity of the gas of interest. Thus, $Sc=n/D$, and D is calculated through Graham's law as,

$$D = n\,(Wa / Wp)^{0.5}\ . \tag{5c}$$

At core of these surface exchange parameterizations is an exchange velocity often referred to as the 'deposition velocity' (V_d). In the bi-directional atmosphere–vegetation exchange, a positive deposition velocity indicates deposition from the atmosphere to the surface while a negative V_d can be interpreted as an emission from the surface to the atmosphere. Thus deposition velocity is a convenient way to parameterize surface–atmosphere exchange for use in analytical as well as numerical models at a regional scale. Deposition flux (F_d, which is the amount of deposited material per unit area for unit time) is defined as the product of V_d with concentration, C, of the depositing material, yielding,

$$F_d = V_d\ .\ C\ . \tag{6}$$

Equation (6) is useful, as deposition velocity estimates are available in literature and often known to be varying over a small range under similar conditions. Knowing ambient pollutant concentrations through measurements (see for example, Padro [45]) or by using air quality models (e.g., Chang et al. [46]), and by prescribing deposition velocity

Mesoscale Atmospheric Dispersion, 2001, Ed. Z. Boybeyi, WIT Publications, Southampton, UK, Advances in Air Pollution, Vol 9, p. 424.

from look-up tables (e.g., Sehmel [47], Voldner [48]) or using dynamic formulations-described ahead, deposition flux can be estimated.

2.2 Obtaining deposition velocity

One way of developing a look-up table for V_d values is using observations based on micrometeorological considerations. Studies such as Duyzer and Fowler [49], Erisman et al. [50], and Erisman and Baldocchi [51] outline different measurement techniques adopted for measuring gaseous deposition. The different micrometeorological techniques are categorized as eddy correlation, gradient, variance, conditional sampling, and eddy accumulation methods. Additionally, surface analysis methods are adopted particularly for complex terrain, in which snow analysis, throughfall, and leaf wash techniques are included. Finally for specie specific studies, chamber techniques are often used. Each of these techniques however, has significant limitations. Erisman et al. [50] discusses these limitations and uncertainties in detail. However, for a homogeneous surface, both F_d and C can be measured with a fair degree of certainty using different approaches (cf. Arya [52], [53], Pleim [54]). If the measurements are made over an extended period (few weeks) and under different seasons as well as environmental conditions (such as wetness, radiation, and temperature) a sufficiently realistic range of V_d values can be obtained. These values can be prescribed for similar landscapes in air pollution models for developing deposition flux estimates. Typically, the concentration estimates are made using a simple gaussian plume model, and the deposition flux is obtained from multiplying concentrations with V_d value [52], [53]. However, measurements have significant uncertainties and are limited in the range of data and variability in the atmospheric conditions (see Brook et al. [55], Niyogi et al. [56]). Hence there is a continued need for parameterizations that can accurately estimate deposition velocities both for observational studies and for numerical/diagnostic models [57].

In parameterizing deposition velocity, often the resistance pathway described earlier is further extended (e.g., Garland [58]). As can be inferred, higher the resistance for the material to deposit, lower will be the deposition flux. Also, following eqn. (6), the deposition flux is directly proportional to deposition velocity. Combining these two features, one obtains deposition velocity as the inverse of total resistance (similar to the approach obtained in eqns. (1) through (6)). For a natural vegetative landscape, the resistance can be offered through different pathways. First, the material has to be dispersed to the receptor surface, then it has to penetrate the quasi-laminar surface boundary layer, and then it has to be captured by the vegetative surface. At the vegetated surface the material encounters resistance from leaf cuticles, stomata, mesophyll, and the soil surface [1]. These resistance pathways can be represented by a total resistance (R_T), comprising of turbulent aerodynamic resistance [*Ra*], surface quasi-laminar boundary [*Rb*], and surface resistance [*Rc*], and can be linked to deposition velocity as,

$$V_d = (R_T)^{-1} = (Ra + Rb + Rc)^{-1} \qquad (7)$$

A schematic representation of the three resistances involved in surface deposition is shown in Fig. 1. Of the three resistances, *Ra*, calculations are independent of the type of gase (see Wesley [24]). *Rb* calculations however, need to consider molecular diffusivity of the depositing gas, and *Rc* estimates show dynamic variations for biophysiochemical responses. We will, therefore, discuss parameterizations for *Rc* in more detail. Also of the three resistances, the *Rc* term is generally dominant, typically by an order of magnitude in various cases (see Baldochi et al. [34], Lynn and Carlson [59]). Following Niyogi and Raman [1], and Niyogi et al. [60], [61], [62] the parameterization approaches can be conveniently classified as ‘environmental’ and ‘physiological’.

In the ‘environmental’ approach, the resistance pathways are modeled as a function of environmental variables such as humidity, surface radiation, and temperature, treating the biospheric components in a parametric form (either through constants or functional entities). In the ‘physiological’ approach, on the other hand, both the environmental and biospheric components are treated as interactive variables. Mathematically, in the environmental approach, the vegetation is treated as a parameter and its role in the mass/energy balance is considered only implicitly, while in the physiological representation, vegetative processes are treated more causally and as a component of the conservation and mass/energy balance equations explicitly [63]. Figure 2, based on Niyogi et al. [60] shows the schematic representation of the two approaches. A similar control between external (environmental) and internal (physiological) parameters on the canopy resistance was developed by Lynn and Carlson [59] using water stress as the driver.

Mesoscale Atmospheric Dispersion, 2001, Ed. Z. Boybeyi, WIT Publications, Southampton, UK, Advances in Air Pollution, Vol 9, p. 424.

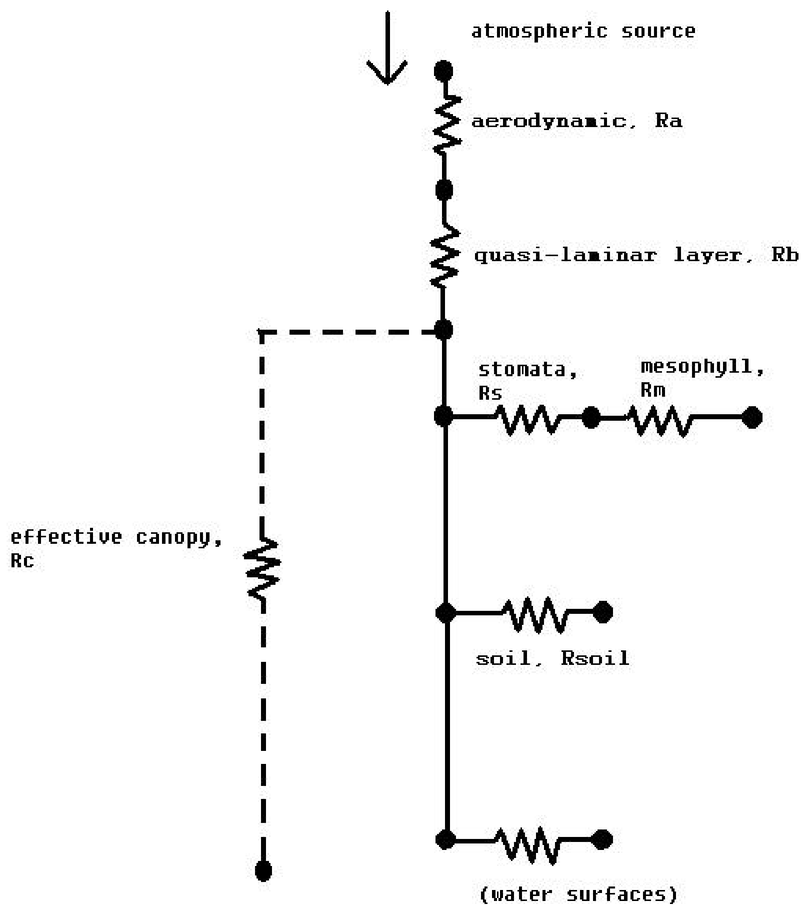

Figure 1: Resistance pathways for depositing material. *Ra* is the aerodynamic resistance, *Rb* is the resistance offered by the quasi-laminar layer close to the depositing surface. *Rc* is the effective canopy or the surface resistance. *Rc* is generally dominant and can comprise of various different resistances before the material deposits. *Rc* dynamically responds to gas characteristics, environmental, and meteorological feedback as well changes in the vegetation canopy.

Mesoscale Atmospheric Dispersion, 2001, Ed. Z. Boybeyi, WIT Publications, Southampton, UK, Advances in Air Pollution, Vol 9, p. 424.

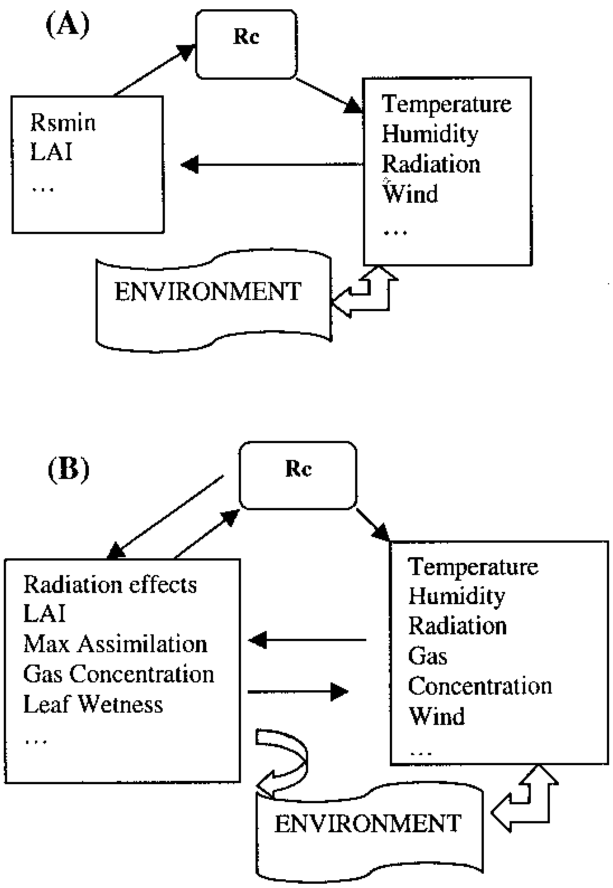

Figure 2: Schematic representation of the (A) Meteorological, and the (B) Physiological pathways for parameterizing the canopy/ surface resistance (*Rc*) term for estimating depositing velocity (*Vd*). In the physiological parameterizations there is explicit feedback interactions between the environment and the depositing surface (foliage).

Mesoscale Atmospheric Dispersion, 2001, Ed. Z. Boybeyi, WIT Publications, Southampton, UK, Advances in Air Pollution, Vol 9, p. 424.

2.3 Environmental Approach for parameterizing V_d

Following eqn. (6), to parameterize V_d, one needs to develop sub-models for the *Rc* term. In estimating *Rc*, all the additional surface resistance (as in eqn. 8) need to be integrated. A central approach of the environmental method for estimating *Rc* was proposed in a seminal work by Jarvis [64]. The surface stomatal resistance was parameterized as a function of the so-called 'minimum stomatal resistance' (R_{smin}), modulated through atmospheric variables such as temperature, radiation, water stress, and humidity. R_{smin} is the minimum resistance the vegetation offers for water vapor exchange. Typically, afternoon values of stomatal resistance in the absence of moisture stress can be considered to be 'minimum' (see Niyogi et al. [65], Avissar et al. [66]). R_{smin} varies according to the vegetation and the season and a typical value of R_{smin} for grassy type vegetation is around 50 s m^{-1}. A detailed review regarding the R_{smin} values for various plant species can be found in Schulze et al. [67] as well as in Kelliher et al. [68]. The Jarvis–type approach has thus become a primary evapotranspiration-stomatal resistance parameterization at all scales. [See for example, Alapaty et al. [69], Wetzel and Chang [70] and Dickinson [71], for modeling studies from micro–to global scales].

The principal equation for the Jarvis-type scheme can be stated as follows (see Noilhan and Planton [72]):

$$R_s = \frac{R_{s\,\min}}{LAI.F_1.F_2.F_3.F_4}\,, \tag{8}$$

where R_{smin} and leaf area index (*LAI*) are prescribed variables, while

$$F_1 = \frac{1+f}{f + R_{s\,min}/\,R_{s\,max}}\,, where,\, f = .55\,\frac{G}{G_l}\,\frac{2}{LAI}\;, \tag{9a}$$

$$F_2 = \begin{cases} 1,\, if\,(w_2 > 0.75 w_{sat}) \\ \dfrac{w_2 - w_{wilt}}{0.75 w_{sat} - w_{wilt}}\;,\, if\,(w_{wilt} \le w_2 \le 0.75 w_{sat})\;, \\ 0,\, if\,(w_2 < w_{wilt}) \end{cases} \tag{9b}$$

$$F_3 = 1 - 0.025.D \,, \qquad (9c)$$

$$F_4 = 1 - 1.6X10^{-3}(298.0 - T_a)^2 \,. \qquad (9d)$$

In the above, G is the net radiation reaching the foliage, G_l is the radiation limit at which photosynthesis is assumed to start (about 100 W m^{-2} for crop-like vegetation). Similar to R_{smin}, it is necessary to prescribe the maximum stomatal resistance (R_{smax}) the foliage can practically offer, and it is generally set at a constant value of 5000 s m^{-1} (see Niyogi and Raman [1], Schulze et al. [67], Kelliher et al. [68]). In the F_2 term (eqn. 9b), w_2 is the deep soil moisture (at 1m below the surface) and w_{wilt} and w_{sat} are the wilting and saturated soil moisture values for the soil (see Clapp and Hornberger [73], Cosby et al. [74], and Noilhan and Planton [72]). Of the remaining terms, D is the vapor pressure deficit given by [$e_{sat}(T_s) - e_a$)]; where $e_{sat}(T_s)$ is the saturated vapor pressure at the surface temperature *Ts*, and e_a is the vapor pressure at the ambient temperature T_a.

Several other forms have been proposed. Wesley [24] adopts one such. In their formulation, it is assumed that stomatal resistance is principally controlled by solar radiation giving,

$$R_s = R_{smin} \,.\, D_{hx} \,[1 + \{200/ (G + 0.1)\}^2 \,]\,[400 / T_a\,(40 - T_a))] \qquad (10)$$

where D_{hx} is the ratio of the diffusivity of water vapor to that of the gaseous pollutant in air. Typical values of D_{hx} for some pollutants are 1.9 for sulfur dioxide and vaporous nitric acid, 1.6 for ozone, carbon dioxide, nitrogen dioxide, and nitrous acid, 1.4 for hydrogen peroxide, and 1 for ammonia.

In addition to the R_s calculations, other resistance pathways (such as cuticular, mesophyll) still need to be estimated. A popular choice for developing the different resistances for vegetated surface is given by Wesley [24] and Walmsley and Wesley [75]. *Rc* is considered to be a combination of stomatal (s), mesophyll (m), upper canopy leaf cuticle (lu), gas phase transfer through convection (dc), lower canopy (cl), canopy height and density (ac), and ground surface (gs) resistances. Thus,

$$Rc = [(R_s + R_m)^{-1} + R_{lu}^{-1} + (R_{dc} + R_{cl})^{-1} + (R_{ac} + R_{gs})^{-1}]^{-1} \qquad (11)$$

In the above, *Rs* can be calculated following eqns. (8, 9 a-d, and 10). The mesophyll acts as an interface for the gases to react with the foliage humidity and the resistance of this exchange is dependent on the gas kinetics alone. Hence a gas reactivity based resistance pathway is adopted, as the gases pass through mesophyll:

$$R_m = (H / 3000 + 100 . f)^{-1} . \qquad (12)$$

In eqn. (12), *H* is the Henry's law constant and *f* is the reactivity factor for the gas. For relatively inert gases such as sulfur dioxide, ammonia, and nitric oxide $f = 0$, for moderately reactive gases such as nitrogen dioxide, and nitrous oxide, $f = 0.1$, and for reactive gases such as ozone, and hydrogen peroxide, Wesley [24] suggests, a value of $f = 1$. The cuticular resistance term (R_{lu}) is calculated in a manner similar to the mesophyll resistance. For a dry surface,

$$R_{lu} = R'_{lu}. (10^{-5} . H + f) . \qquad (13a)$$

In this calculation, R'_{lu} is a default resistance factor assigned as a function of landscape (land use) and the season (see Wesley [24]). Typical values range from 2000 s m^{-1} in midsummer for green vegetation to about 9000 s m^{-1} during winter. The cuticles due to their functional role in plant transpiration are highly responsive to moisture availability. Hence the cuticle resistance also changes significantly due to variations in surface wetness (see Fuentes and Gillespie [26]). Under humid conditions, the cuticle resistance is largely controlled by the hygroscopic properties of the exchanging gas. Wesley [24] suggest an adjustment as, $R_{lu}=[1/W+1/(3R_{lu})]^{-1}$. Considering ozone for instance, the resistance value (referred to as R_{luo}) under moderately wet conditions, such as dew formation, can be calculated with W = 3000 and with W = 1000 for rain wetted conditions. Wesley [24] provides another limit specifically for sulfur dioxide transfer. For this, they suggest R_{lu} as 100 s m^{-1} for dew wetted conditions and 50 s m^{-1} for urban regions. Additionally, W is assigned a value of 5000 for the rain event. For any gas other than sulfur dioxide and ozone, in wet conditions, use of the following equation, is suggested:

$$R_{lu, wet} = [1 / (3 R_{lu,dry}) + 10^{-7} H + f / R_{luo}]^{-1} . \qquad (13b)$$

Sutton et al. [76] proposes an alternate general formula, based on different laboratory and field measurements. They consider relative humidity (*rh*) control on the resistance, which is more convenient to model rather than dew and rain. They propose:

Mesoscale Atmospheric Dispersion, 2001, Ed. Z. Boybeyi, WIT Publications, Southampton, UK, Advances in Air Pollution, Vol 9, p. 424.

$$R_{lu} = 2 \exp ([100 - rh]/12) \,. \qquad (13c)$$

The depositing matter has to encounter two additional resistances, namely the lower canopy (R_{cl}) and the ground surface (R_{gs}). Typically, the resistance values for both ozone and sulfur dioxide are of the order of 200 s m^{-1} for the ground surface and of the order of 1000 s m^{-1} for the lower canopy resistance. Using these resistance values for sulfur dioxide and ozone, more generalized formulae for the resistances are derived, yielding:

$$R_{clx} = [\, H /(10^5 .\, R_{cls}) + f / R_{clo}]^{-1} \,, \qquad (14a)$$

$$R_{gsx} = [H / 10^5 \, R_{gss}) + f / R_{gso}]^{-1} \,. \qquad (14b)$$

Based on several observations, it is recognized that surface temperature has a significant control over the cuticular, lower canopy, and the ground surface response to depositing matter. For lower temperature, Walmsley and Wesley [75], suggest a correction term $R_{low}=10^3.exp(-Ta-4)$, to be added to the resistance such as R_{lu}, R_{cl}, and R_{gs}.

Finally from eqn. (10), the buoyant–convection resistance is a function of radiation and the slope of the terrain (ϑ, in radians) and is estimated as, $R_{dc}=100[1+1000(G+10)^{-1}].(1+1000J)^{-1}$. The slope can be conveniently assumed to be zero in a regional scale analysis [43], [44]. Knowing the different resistances, surface–atmosphere exchange fluxes can be obtained (cf. Kramm et al. [38]), by explicitly representing the vegetation–atmosphere exchange (F_f) and the ground surface and the atmosphere flux (F_g):

$$F_f = - [(c_f - H.c_{int}).\, (R_s + H.R_{int})^{-1} \,] - [(c_f - c_{cu}).(R_{cu})^{-1} \,] - [(H.R_{wf})^{-1} \,.\, (c_f - H.\, C_{wf})] \,, \qquad (15a)$$

$$F_g = - [(c_g - H.c_{wsl}).\, (H.R_{wsl})^{-1} \,] - [(c_g - c_{sl}).(R_{sl})^{-1} \,] \,. \qquad (15b)$$

In the above equations, *c* and *C* refer to surface and aqueous state concentrations, and subscripts *f*, *int*, *cu*, and *g* correspond to the foliage, intercellular cells, cuticle, and ground surface levels respectively. *H* is the Henry's law constant, *R* is the resistance offered to the exchange, while the additional subscripts, namely, *wf*, and *wsl* refer to the wetness at foliage, and the soil surface. An alternate deposition flux parameterization involving K-theory along with a vegetation canopy–

Mesoscale Atmospheric Dispersion, 2001, Ed. Z. Boybeyi, WIT Publications, Southampton, UK, Advances in Air Pollution, Vol 9, p. 424.

atmosphere interface can be found in Underwood [77]. Note that since the resistance is function of the surface they represent (vegetation or ground), it has to be normalized by the surface area. For a grid, this can be normalized by vegetal cover fraction (*veg*). Thus for the foliage the effective resistance will be obtained by normalizing through *veg*, and the soil resistances by (1-*veg*).

An important aspect for operational models is that it is only the *net effect* (combined resistances of all the vegetative and surface parameters) that is required (as R_c) in estimating V_d. Hence, while designing the gas exchange system, one can either approach it in the detailed analysis as eqn. (11), or represent the R_c term by scaling the R_s over the entire canopy through LAI. Thus most models adopt,

$$R_c = \Sigma R_s \,.\, LAI. \quad (16a)$$

Further, to account for the differences in the surface characteristics due to vegetal cover, the effective R_c can be represented as,

$$1 / R_{c,eff} = veg / R_s + (1\text{-}veg)/ R_{soil} \,. \quad (16b)$$

Knowing R_a, R_b, and R_c, gas deposition fluxes can be obtained.

One of the effects of the material deposition is that it reduces the material to be dispersed further downwind. This can be adjusted through a net reduction in the mass transfer over the grid boundaries or as an effective reduction in the emission source strength for subsequent time steps (see Horst [78], Arya [53]).

3 Terrestrial biosphere as a source and sink

One of the limitations of the approaches and formulations presented until now is that they do not explicitly account for the changes in the source/sink relationship discussed earlier. As observed with the biogenic VOCs, for example, the resistance pathways need to be designed for bi–directional exchanges so as to be generalized. To address this issue, recent efforts are directed towards the development of modified flux emission–deposition approaches that would account for bi-directional exchanges. We will discuss this issue, using of two recently published studies as examples: Xu et al. [29] and Sutton et al. [79]. The Sutton et al. [79] study focuses on the traditional bi-directional issue namely that of the 'ammonia compensation point' (see Farquhar et al. [80], [81]). Ammonia can be efficiently deposited to moist surface and get converted to ammonium. However, the leaves themselves generate ammonium radicals in plant tissues. This ammonium can be subsequently dissociated resulting into ammonia release in substomatal cavity. Such a compensating scenario can lead to an equilibrium in the direction of the mass flow (emission or deposition), depending on the ambient pollutant concentration. We will review this issue in more detail because of its importance for the development of bi-directional exchange models. The Xu et al. [29] work on the other hand, is of interest, because it deals with a regional scale application of mercury emission and deposition and is based on regression equations-based flux assumptions. Thus it differs from the more mechanistic 'compensation point'–based studies.

Hanson et al. [82] provides an observational evidence of the bi-directional flow of the mercury mass exchange in the terrestrial ecosystem. The starting assumption of the regression–based models, such as Xu et al. [29], is that there is a non-causal relation between evapotranspiration and surface emission. Following this assumption, a biogenic/surface pollutant (mercury) emission rate (*Fc*) can be assumed, as a product of surface evapotranspiration (*Ec*), and pollutant concentration (*Cs*) at the surface soil solution, $Fc = Ec.Cs$. Interestingly, a similar approach was recently successfully adopted by Pleim et al. [54] to develop deposition estimates from field observations. Under wet and unstressed conditions, the evapotranspiration is assumed to be small and the vegetation is conducive for deposition.

Ec can be estimated from routine climatic information (temperature, humidity, and rainfall, see Mahfouf [83]) or from detailed micrometeorological observations (see for example, Pleim et al. [54]). Additionally, *Ec* can be estimated using detailed soil–vegetation–atmosphere-transfer (SVAT) models such as that of Deardorff [84], Noilhan and Planton [72], Alapaty et al. [69], Wetzel and Change [70, and Xue et al. [85] that are embedded in different mesoscale and regional scale models. Alternatively empirical relations such as the Penman–Monteith equation (see Acs [86], and Monteith and Unsworth [87]) can be used to develop *Ec* estimates. Xu et al. [29], for instance, used the Penman–Monteith relation for estimating *Ec* along with a soil-water-deficit factor of Raupach [88]. They estimate *Rc* as (R_{smin} / f_m), where f_m is a function of soil water deficit (*M*). For values of *M* between 0 and 5 cm of water, f_m is 1, for M greater than 20 cm of water, f_m is 0. For intermediate ranges of M, f_m is linearly scaled as (20– M)/15. In addition to this transpirative control of pollutant emission, the regression-based models also relates soil surface emissions using surface variable such as soil temperature, radiation, and soil moisture status. In their study, Xu et al. [29] adopt a regression model based on Carpi and Lindberg's [89] observations. They develop an equation of the form, $log(F_{soil})=a.(T_{soil})+b$. The coefficients a and b are hypothesized to be a function of surface characteristics such as soil wetness. In the case of mercury for instance, Xu et al. [29] use values of a = 0.057 and 0.064, and b = -1.7 and –2.03. Concurrently, the deposition flux is obtained by estimating V_d as discussed earlier. Their results show some typical features that are of relevance to mesoscale models. First, there is a strong diurnal variability in both the emission as well as the deposition rates. Second, the transfer velocities for emission as well as deposition, are coupled with land–use pattern. This difference is principally due to the variations in the *Rc* term as a function of the vegetation/surface changes. The deposition rate was about 10 % of the emission for agriculture landscape. This increased to about 15 to 20 % for urban areas and about 20 % for forests. As discussed earlier, the availability of surface moisture has a profound impact on deposition estimates (see Harley et al. [90]). For mercury, Xu et al. [29] estimate a 11 % change in the area averaged dry deposition for 1 % wet surface.

Though in this study, the model processes are not causal in their formulation, they serve as an example as to how data from field experiments can be adopted in developing regional scale scenario evaluation for air–surface exchanges (see Lemon and van Houtte [91]). Indeed it is possible to develop statistical–dynamical couplings for other terrestrial emissions such as isoprene, monoterpenes, and different nitrogenous compounds. These models are also computationally efficient due to their analytical form and simplicity. An additional feature is that such models allow an easier interpretation of the cause–effect relationship often sought for policy development [65].

However, there are some limitations, when dealing with such statistical–dynamical relations. One, typically they cannot help develop a general scenario, as the range over which they can be applied could be fairly limited. The range over which observations were available for developing such regression relations generally sets these limits. Two,

Mesoscale Atmospheric Dispersion, 2001, Ed. Z. Boybeyi, WIT Publications, Southampton, UK, Advances in Air Pollution, Vol 9, p. 424.

these relations are developed from observations which can have a significant error bar (sometimes of the same order of magnitude as the mean observed value itself, see for example, Fowler et al. [92]). This introduces significant uncertainty in the results. Dynamical processes can be fairly compensatory over a wide range, while in the statistical relations the uncertainty persists (cf. Niyogi et al. [56]). Third, the functional form used in developing the relations can make the system biased towards emission or deposition, and thus create a difference in the direction of the mass flow. As an example, the Xu et al. [29] study, adopts the use of logarithm in emission term, making it biased for positive values, namely emissions as against deposition. Fourth, unless explicitly specified, the statistical models often cannot account for effects of co-varying or second order interactions in the environmental system [93]. For instance changes in the basal characteristics of the biogen such as the emission rate (e.g., Monson et al. [94]), or seemingly contrasting changes in the physical characteristics (such as increased radiation as well as humidity, increased air temperature and lowered foliage temperature) can lead to very different results in the modeled outcome and reality (see Nikolov et al. [95]).

For such reasons, the 'compensation point' approach [80], [81], [82] appears more encouraging for developing bi-directional models. A study by Sutton [79] which develops and applies the bi-directional exchange for ammonia is discussed here. As discussed earlier, due to the physiological emission of the ammonium radicals and their subsequent dissociation form ammonia, the concentration flux can vary its direction and magnitude significantly [96]. Indeed a similar case can be made for mercury and several other VOCs.

Following eqns. (1) and (7), gradients in the surface concentrations can be used for estimating surface fluxes. As a first approximation, Sutton [79] assume that the surface concentration is zero and that the gas concentration at reference level can yield a gradient for calculating the fluxes. These fluxes can be linked with total resistance (R_T) following eqn. (7). Then *Ra*, and *Rb* can be calculated following eqns. (3), (4), and (5). Knowing R_T, *Ra,* and *Rb*; *Rc* is obtained as a residual resistance term. This *Rc* is then used with other meteorological and chemistry datasets (observed or modeled) to generate corresponding flux values. Meyers and Paw [97], as well as Meyers and Baldocchi [98] used a similar approach both with observations as well as vegetation models. However in their study for nitric acid deposition, they assume a zero resistance from the canopy for exchanges between the surface and the overlaying atmosphere.

Indeed such approaches do not provide a mechanistic feedback between physiological changes and the environment. However it can provide a better analysis mode for bi-directional fluxes for specialized fields experiments in which detailed observations are available against which robust regression models can be generated. To introduce the physiological feedback, the resistance terms can be linked to yield a compensation concentration point (C_{cp}),

$$C_{cp} = Cr + F_i \,.\, (Ra + Rb)\,. \qquad (17)$$

Using the compensation point as a central parameter rather than Rc, a flux–resistance approach can be developed.

Total flux has to be conserved between cuticle (F_{lu}) and the stomata (F_s). This yields, $F_w=C_{cp}/R_{lu}$ and $F_s=[C_{cps}–C_{cp}]/R_s$, where C_{cps} is the compensation point for the stomata (rather than the canopy), and is calculated similar to eqn. (17) as, $[Cr+F_i.(Ra+Rb+Rs)]$. The cuticle resistance can be estimated from eqn. (13 a, b, c), and a generalized compensation point can be obtained as,

$$C_{cp} = \frac{\lfloor C_r / (R_a + R_b) + C_{cps} / R_s \rfloor}{\lfloor (R_a + R_b)^{-1} + R_s^{-1} + R_w^{-1} \rfloor}. \qquad (18)$$

In eqn. (18), the effect of soil emission can be introduced by simply adding one more soil flux term (F_{soil}) in the numerator (see Sutton et al. [99]). It is important to note that the soil flux term added thus will not be a constant background type additive correction to the bi–directional flux model (see Carpi and Lindberg [89]). Since the flux is introduced in a manner similar to altering the resistance, there will be feedback in the leaf surface/stomate and the soil exchanges. Indeed such an additive flux emission is a simplification and more explicit and detailed representation may be necessary for regions in which soil surface emissions are dominant [89]. One example of such a case could be an animal waste site in agricultural utility regions. Since by definition, at compensation point there will not be any mass exchange, eqn. (18) can be simplified to yield,

$$C_{cp} = \frac{C_{cps}/R_s}{R_s^{-1} - R_w^{-1}}. \tag{19}$$

Using eqn. (18), Sutton et al. [79] obtain results that agree well with observations for bi–directional flux transport over a wheat canopy. Though the above example is not unique and other researchers have proposed similar exchange models even within a gaussian plume framework (see for example, Asman [100]), two features deserve additional mention. First, the example demonstrates a method in which the existing deposition velocity–resistance relations (eqn. 6) can be conveniently modified to configure the bi-directional exchange within the modeling system. This can be achieved at a landscape as well as at a regional scale. Second, leaf and canopy scale processes have profound impact on the landscape flux characteristics. Related to the leaf scale control issue, several studies such as Rondon and Granat [101], Monson et al. [94], and Schjoerring et al. [93], for instance, provide observations on the physiological control of plant–atmosphere exchange. They find convincing evidence that stomatal conductance (inverse of resistance) controls the exchanges; and physiological variables such as foliage temperature, for instance, couples tightly with the exchange fluxes. The models discussed so far, have an advantage that they represent the modeling process within the traditional meteorological/environmental approach itself (see Fig. 2). For bi–directional exchanges, due to their very nature, models are needed to explicitly account for the physiological responses. Efforts are underway to couple biological processes with meteorological models thus giving an opportunity to develop realistic surface–atmosphere exchange modules. In the following section, we will discuss these model formulations in more detail.

3.1 Biosphere atmosphere exchanges by physiological approach

As described in Niyogi and Raman [1] and Niyogi et al. [60], for the environmental Jarvis-type schemes, it is the ambient environment or the meteorology that is a dominant factor, in determining the stomatal resistance. Lack of physiological feedback may be valid for various routine field situations. However, there is increasing evidence that the physiological feedbacks in the form of biochemical stimuli or plant

Mesoscale Atmospheric Dispersion, 2001, Ed. Z. Boybeyi, WIT Publications, Southampton, UK, Advances in Air Pollution, Vol 9, p. 424.

photosynthesis are a requisite causal indicators of the stomatal activity terrestrial exchange. Here we discuss the physiological Gas exchange and surface Evapotranspiration Model (GEM) developed by Niyogi et al. [28], [61], [62], [103] and Niyogi and Raman [102].

GEM considers *Rc* as a combination of various resistances at the surface (vegetated or bare soil), to yield an areal average for each grid point in the numerical model,

$$Rc = (1\text{-}veg)\, Rsoil + (veg)\, Rs \,. \qquad (20)$$

Unlike the meteorological/environmental formulations, *Rs* is taken as a continuum between soil thermal and hydraulic feedback in terms of the surface energy and soil moisture balance, and the canopy processes. The model considers mechanistic leaf scale gas assimilation/ photosynthesis, evapotranspiration and energy balance, along with a dynamic link with the atmosphere through mass and energy transfer as well as gas exchange (cf. Cowan [63], Elssworth [104], Niyogi and Raman [1]). The logical flow in GEM is as follows: stomatal resistance (r_s) is inverse of stomatal conductance (g_s); conductance is known to correlate with carbon assimilation or photosynthesis (A_n) (cf. Wong [105]); and the photosynthesis is dependent on the biophysiochemical state of the foliage and its surrounding environment such as carbon dioxide at surface (C_s), within the leaf cells (C_i), and humidity at leaf surface (rh_s) (cf. Farquhar et al. [81], [106], Farquhar and Sharkey [107]).

In GEM, stomatal conductance (g_s) is estimated following the Ball-Woodrow-Berry model (see Ball [108], [109], Niyogi and Raman [1] as well as a critique by Aphalo and Jarvis [110], Mott and Parkhurst [111], and Monteith [112], [113]). Accordingly,

$$g_s = [m \,.\, A_n .\, rh_s \,/\, C_s] + b \,. \qquad (21)$$

Photosynthesis or carbon assimilation [11], [114], [115], is taken as the residue of gross carbon assimilation (A_g) and loss due to respiration (R_d). A_g is taken as the weighted minimum of three limiting functions, namely, assimilating efficiency of photosynthetic enzymes (Rubisco limited; w_c), radiation (w_e), and carbon dioxide (w_s) (see Collatz et al. [116], [117]). Giving,

$$w_c = V_m \;, \qquad (22a)$$

Mesoscale Atmospheric Dispersion, 2001, Ed. Z. Boybeyi, WIT Publications, Southampton, UK, Advances in Air Pollution, Vol 9, p. 424.

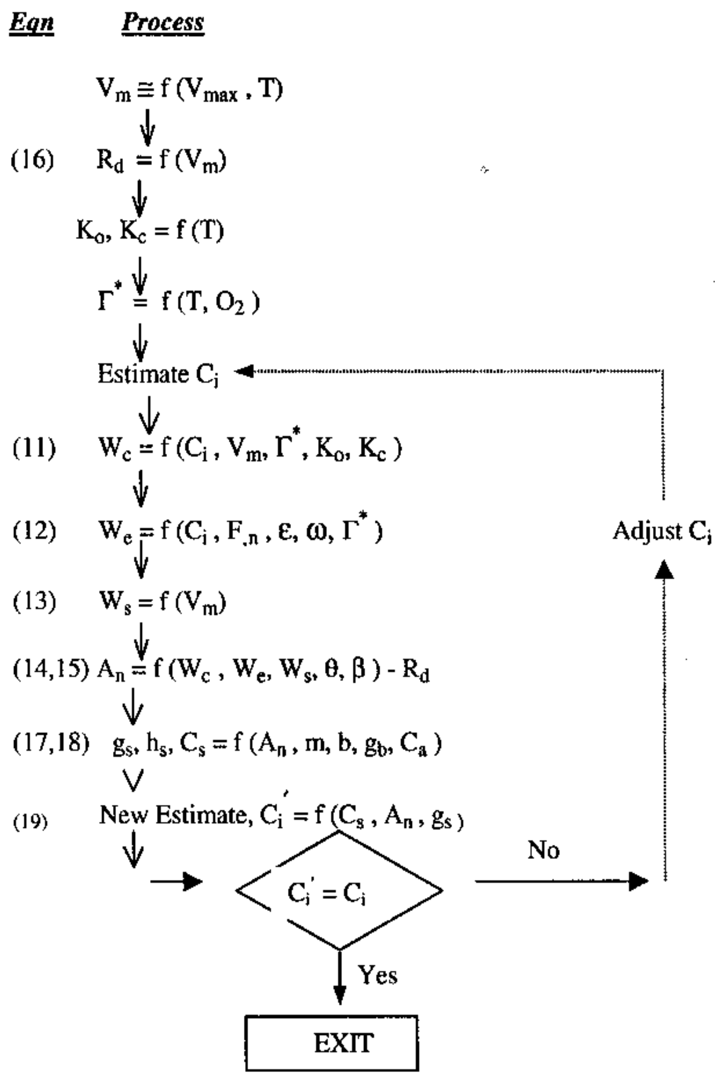

Figure 3. Flowchart showing the decision process in solving the iterative $g_s - A_n$ equations in GEM. (Based on Sellers et al. [125], Su et al. [127], Niyogi et al. [102])

$$w_e = PAR.e.(1 - w_p) \ , \tag{22b}$$

$$w_s = \frac{20000.V_m.C_i}{P} \tag{22c}$$

where e is the intrinsic quantum efficiency for corbon dioxide uptake, and ω_π is the leaf-scattering coefficient for photosynthetically active radiation (PAR, see Sellers et al. [118], Niyogi et al. [61], [62]). V_m is estimated as a function of soil moisture and ambient temperature [117], [119]. P is the atmospheric pressure, which is prescribed or obtained as a tendency term in the meteorological model, and *PAR* is calculated following Noilhan and Planton [72] as function of net radiation. Knowing w_c, w_e, and w_s, corresponding smoothed minima (cf. Collatz et al. [116]) gives the gross primary productivity (A_g). Knowing A_g photosynthesis (A_n) can be calculated by taking off the loss in resources due to respirative processes (R_d). Following Collatz et al. [116], R_d can be taken as certain percentage (1.5 to 2.5 %) of V_m. Another approach developed and presented in Goudriaan et al. [120], Kim and Verma [121], van Heemst [122], Jacobs et al. [123], and Calvet et al. [119] is also available. Accordingly, R_d is parameterized as 0.11 A_m, where, A_m (or $A_{m,max}$) is the maximum assimilation rate [67] limited through carbon dioxide deficit (see Jacobs et al. [123], Jacobs [124]), and mesophyllic conductance (g_m) as,

$$A_m = A_{m,max}\,[1 - exp(-g_m(C_i - G) / A_{m,max})] \ , \tag{23}$$

g_m is parameterized following Calvet et al. [119], and Niyogi et al. [61], [62],

$$g_m = g_{m,max}(2^{Q_t})\left[\frac{1 + exp(0.3(T_c - S_2))}{1 + exp(0.3(S_1 - T_c))}\right].\left[\frac{(w_2 - w_{wilt})}{(w_{sat} - w_{wilt})}\right] \tag{24}$$

In the above, $g_{m,max}$ is typically of the order of 17.5 x 10^{-3} m s^{-1}, S_1 and S_2 are landuse based temperature coefficients. Sellers et al. [125], [126], provide look-up tables for these coefficients as a function of vegetation type. *Tc* is the surface temperature, and w_2, w_{wilt}, and w_{sat} are the deep (root level) soil moisture, and the wilting and saturation capacity of the soil. All the variables are either specified as a function of the landuse or determined prognostically in the SVAT module in GEM. Obtaining g_b, the carbon dioxide concentration at the leaf surface (C_s) can be estimated following Su et al. [127] as,

$$C_s = C_a - \frac{A_n}{g_b} . \tag{25}$$

From eqn. (25) a first estimate of g_s is made. Closure is obtained by estimating C_i as,

$$C_i = C_s - \frac{D_{hx} . A_n P}{g_s} . \tag{26}$$

D_{hx} is the diffusivity ratio to accommodate for different gases, as discussed earlier [24]. The set of equations is solved in an iterative mode till a convergence is achieved. Finally in GEM, a lag is introduced for the changes between (from or to) physiological and the ambient environment (see Jones [128] for observations and Su et al. [127] for large eddy simulation results). Accordingly the temporal stomatal response $g_s(t)$ for the steady state stomatal conductance, g_s, is introduced based on the stomatal conductance value for the prior time step $g_s(t\text{-}1)$ giving,

$$g_s(t) = g_s(t-1) + [\, g_s - g_s(t-1)] \times [1 - exp(-k(Dt/t)] . \tag{27}$$

GEM and similar modules (SiB2 [125], CANVEG [129], [130], IBIS [119]) can be efficiently coupled to any PBL or mesoscale model through surface energy balance and SVAT [1], [69], [72], to achieve complete integration. Figure 3 shows the process flow chart for the physiological terrestrial atmosphere exchange. In GEM, the Ball–Berry model for the g_s–A_n relation is used. Niyogi and Raman [1] review additional physiological approaches, one of which is vapor pressure deficit (D)-stomatal conductance (g_s) and – carbon assimilation (A_n) analytically relation of Jacobs et al. [123]. Calvet et al. [119] describe a recent application of such a model and a summary is presented here.

The gas (water vapor) exchange parameterization is efficiently linked with a stomatal conductance model through gas concentrations and a canopy scaled conductance. They use the following equation:

Mesoscale Atmospheric Dispersion, 2001, Ed. Z. Boybeyi, WIT Publications, Southampton, UK, Advances in Air Pollution, Vol 9, p. 424.

$$G_s = g_s^* + E\ M_a / M_v\ .\ (C_s + C_i) / [2\ (C_s - C_i)]\ , \qquad (28a)$$

$$g_s^* = 1.6\ g_{sc}^* + g_c\ , \qquad (28b)$$

$$g_{sc}^* = \frac{A_n - \left(\frac{D_s}{D_{max}} \times \frac{A_n + R_d}{A_m + R_d}\right) + R_d\left(1 - \frac{A_n + R_d}{A_m + R_d}\right)}{C_s - C_i}\ , \qquad (28c)$$

$$C_i / C_s = f + [(1 - f)\ (\Gamma / C_s)]\ , \qquad (28d)$$

$$f = f_o\ (1 - D/ D_{max}) + f_{min}\ (D/D_{max})\ , \qquad (28e)$$

where g_c is the cuticular conductance, M_a, and M_v are molecular masses of air and water vapor, G is carbon dioxide compensation point. This is the CO_2 leaf intercellular concentration, below which, leaf is unable to carry out photosynthesis, due to photorespiration. The compensation point is about 45 ppm for woody trees, and 3 ppm for grassy landscape. Leaf transpiration E is estimated as $r_a g_s D_s$. f_o is value of f for D_s=0, and is of the order of 0.85 for woody trees, and 0.5 for grass. Following Choudhury and Monteith [131], D_{max} is often taken as 45 g kg^{-1}. Using this formulation Calvet et al. [119] find good agreement between observations and predictions for different cases. Indeed some studies [110], [111], [112], [113] question the causality of relative humidity based g_s–A_n relations such as the Ball–Berry model, and prefer the vapor pressure deficit approach (see also Dougherty et al. [132]). In reviewing different g_s formulations Niyogi and Raman [1] and Niyogi et al. [60] conclude that at short time scales (few hours) the two approaches indeed provide different values. Qualitatively both the humidity representations were similar in their functional form and responses, but different in terms of their numerical outcome. These results suggest it is important to choose the canopy resistance scheme appropriately depending on the trace species and their humidity dependence. Further it may be often necessary to independently evaluate the resistance pathways for the trace gas and pollutant, and their successful validation for surface energy balance and meteorological models may not be sufficient criteria for choosing one formulation over another.

Mesoscale Atmospheric Dispersion, 2001, Ed. Z. Boybeyi, WIT Publications, Southampton, UK, Advances in Air Pollution, Vol 9, p. 424.

4 Regional mapping

Until now, we discussed different modeling approaches in the development of deposition and bi-directional fluxes. One of the major issues in including such an analysis for a mesoscale model, is the scaling of the deposition estimates to a regional scale. In this section, we will discuss the application of the various formulations and the techniques used for such scaling.

Studies involving regional mapping of deposition and regional mass balance recognize the limitations of point observations [133]. Most observations are limited in time and space and cannot be efficiently used for generating spatial distributions or maps. This issue is discussed following a recent deposition mapping exercise adopted for the United Kingdom using observational data alone [49].

A literature review is generally necessary for various deposition velocity estimates as a function of measurement techniques, landscape characteristics as well as the pollutant. The reported V_d values for different gases include: nitric oxide ranging from 10^{-4} to 2 mm s^{-1} over soil and about 1 mm s^{-1} over vegetation [134], [135]; nitrogen dioxide from 2 mm s^{-1} over grass [92], 3 to 7 mm s^{-1} for forest surface, as well as sand and clay soils [136], [137], to 13 mm s^{-1} for alfa-alfa grass [4]; peroxy acetyl nitrate (PAN) from 2 mm s^{-1} over grass [9] to 8 mm s^{-1} over alfa-alfa [4], 0.9 mm s^{-1} for acidic moorland to 2 mm s^{-1} over calcareous soil/patchy grass [138]. Erisman and Baldocchi [51] and Erisman et al. [139] summarized recent sulfur dioxide deposition estimates from various studies. They report values ranging from 1 mm s^{-1} to 20 mm s^{-1}, for bare soil to coniferous forests, with the higher values for forest landscape (see also Rondon et al. [140]). Various such measurements are available from field programs though mostly in the U.S. and the Europe. Using these values of V_d, with representative concentration values, deposition fluxes are calculated. These fluxes are then mapped using geographical information system (GIS) based approaches.

Models are still widely used due to lack of observations in many cases. For example, Duyzer and Fowler [49] report absence of PAN observations over forest region, and nitrous acid and resort to using Wesley's [24] model (which yielded a value of 5 mm s^{-1} for PAN and 10 mm s^{-1} for nitrous acid) for the forest landuse. Similarly there is a need to generate diverse climatic scenario for different landscapes since moisture has a major effect on the deposition potential. A typical approach involves following steps. First high-resolution surface features, and emission inventory of the pollutant to be analyzed is generated. The emissions are fed in to an environmental/air pollution–deposition model. The model also requires climatological or prognosticated humidity, precipitation, temperature, winds, and radiation fields [141], [142]. A high-resolution surface data set comprising of vegetation type, soil type, leaf area index, roughness length, and vegetation characteristics is required. The accuracy of the surface data will determine to a large extent, the appropriateness of analyzed and predicted deposition fields. The resulting distributions are generated hourly or integrated over month, season, and year. The generated estimates can be used for mapping the zonal susceptibility (see for example, Singles et al. [143]).

In addition to surface observations, use of satellite data will be beneficial for providing input values for generating mesoscale model based deposition output. While developing the bi-directional models, we discussed the relations between evapotranspiration and the gas exchange fluxes. Taconet et al. [144] present a canopy resistance model based on thermal infrared remote sensed data:

$$R_S = R_{s\,\min}\left[\frac{R_{n\,\max}}{c_1.R_{n\,\max}+Q}+\left(\frac{1.2w_{wilt}}{w_s}\right)^2\right].\frac{1+0.5LAI}{LAI}\,. \tag{29}$$

Here, c_1 is of the order of 0.03, and other variables are similar as described in eqns. (8) and (9). Similarly, Nemani and Running [145] successfully tested the potential of using spectral index-*NDVI* (normalized differential vegetation index) for evapotranspiration and hence *Rc* estimates. Studies such as Asrar et al. [146], for instance, have established the correlation between leaf area coverage and the infrared/red band values [147], [148]. Green leaves, due to the presence of chlorophyll, absorb radiation in red wavelengths. Hence red reflectance (*RED*, 0.55–0.68μ) is negatively correlated with chlorophyll and green vegetation, while the near infrared (*NIR*, 0.73–1.1μ) is scattered by the physiological characteristics of the leaves. *NDVI* is calculated as:

$$\text{NDVI} = [(\text{NIR} - \text{RED}) / (\text{NIR} + \text{RED})]. \tag{30}$$

Nemani and Running [149] obtain a relation between *LAI* and *NDVI* as:

$$\text{NDVI} = [\ln (\text{LAI} / 0.65)] \text{ X } 34 \,. \tag{31}$$

Using this as a starting point, Nemani and Running [145], represent a relation between surface temperature (*Ts*) and NDVI of the form, $T_s = a + b\ NDVI$. For their data they obtained a ranging from 28 to 60 and b from 24 and 45. They refer to the slope of the T_s-*NDVI* best fit as s, and deduce a relation between s and R_c as: $R_c = -\ln(s/48) \times (-10)$.

Additional details regarding such an approach in mesoscale–regional landscape perspective can be found in studies such as Cihlar et al. [150], Seevers and Ottmann [151], and Szilagyi et al. [152]. Indeed, development of R_c estimates allows regional deposition assessment for models. The above approach is attractive as it has direct relevance for biospheric models that seek information regarding surface characteristics from satellite data [126]. In the final section, we will hence describe such a methodology, for R_c estimation with both the Jarvis-type and the physiological g_s–A_n models in perspective [118], [126], [153], [154]. For instance, Sellers et al. [118] proposed,

$$g_s = \left[\frac{b_1 + F.n}{a_1 + b_1 c_1 + c_i F.n} \right] \left[f(T).f(w_2).f(e) \right], \tag{32}$$

where a_1, b_1, c_1 are specie dependent constants. Using different parameterizations (for e.g., Charles–Edwards and Ludwig [155], Jarvis [64], Farquhar et al. [106], and Collatz et al. [116], [117]), Sellers et al. [118] estimate the constants to be 13966, 0.1, and 28 respectively. *F.n* is the normal component of the vector flux for *PAR*, and *f(T), f(w2), f(e)* are the temperature, soil moisture, and vapor pressure deficit, as explained in eqn. (9). The canopy conductance (inverse of resistance), which is used for estimating surface deposition, can be obtained by integrating the conductance over canopy *LAI*. In developing radiometric data based biophysical parameters, in addition to *NDVI* (eqn. 29), Sellers [153] use the Simple Ratio (*SR*) (defined as ratio of *NIR* to *RED*). Under conditions such as uniform canopy, dark soil, and light to moderate water stress following relation can be established:

$$\frac{\partial g_c}{\partial (LAI)} \alpha \frac{\partial (SR)}{\partial (LAI)}. \tag{33}$$

However for physiologically intensive photosynthesis–based schemes, Sellers et al. [118] extend eqn. (32) to yield,

$$\langle g_c \rangle = \frac{1}{S}\int_0^s g_c \, ds \, \alpha < SVI >, \tag{34}$$

where < > refers to area–integral and spatial averages (*S* is area of the region), the and *SVI* is spectral vegetation index such as *SR* and *NDVI*. Thus the adaptation of the spectral indices as obtained through satellite imagery for instance, into mesoscale models will be governed by the type of resistance formulation adopted. In summary, spatial averages of the spectral indices can yield spatial averages of canopy conductance (inverse of resistance). A functional form can be deduced based on leaf biophysical properties (such as radiation limit and V_{max}, see Goudriaan [156]), photosynthetically active radiation (*PAR*) usage over the canopy, and environmental feedback through forcings such as temperatures, humidity, and moisture availability:

$$g_c \equiv [V_{max}, F_o].[\Pi].[F_i]$$

$$g_c \equiv [Leaf\ Properties].[PARUsage].[EnvironmentalFeedback] \tag{35}$$

Additional description on the use of spectral indices for biophysical processes can be found in Asrar [157]. Significant uncertainty has to be assigned due to limitations in spatial resolution, and the heterogeneity of bio-physiochemical as well as radiative properties within model landscape. However, the radiance based approach for a mesoscale air pollution modeling appears to be quite promising for mesoscale deposition analysis.

5 Summary and concluding discussion

We have discussed the role of vegetation and terrestrial biosphere in the mesoscale air pollution systems. Generally the surface acts as a sink and aids gaseous deposition. Accordingly, we discussed the development of different parameterization schemes using a resistance pathway between

Mesoscale Atmospheric Dispersion, 2001, Ed. Z. Boybeyi, WIT Publications, Southampton, UK, Advances in Air Pollution, Vol 9, p. 424.

the aerodynamic, surface boundary layer, and the depositing surface. Such schemes can be categorized under Jarvis–type environmental or meteorological exchange schemes in which the biospheric characteristics are not dominantly interactive. In addition to being a sink, the terrestrial biosphere can also be a significant source for what is referred to as biogenic emissions. Examples include gases such as isoprene, monoterpene (which can be photochemically transformed into ozone), nitrogen compounds, and mercury. Such scenarios provide an impetus for implementation of a generalized bi-directional surface–atmosphere exchange processes in air pollution models. The bi-directional exchange is parameterized principally through development and modification of surface resistance schemes.

Two developments were discussed in which the Jarvis-type environmental approach could be utilized. The first involves adopting a statistical regression equation based estimation of the exchange flux. The second method is based on a 'compensation point' approach. In this, the differences in gas concentration within the canopy (surface) and the air around it determine the direction of flux transport. In addition to the modifications to the Jarvis-type schemes, a physiologically intensive surface–atmosphere exchange was also discussed. In this the exchange is not only controlled by the environmental forcing, but also by the within canopy bio-physiochemical reactions. A methodology for coupling such exchanges in mesoscale air pollution systems was discussed. Finally a critical component of adopting such surface–atmosphere deposition or exchange modules in the mesoscale perspective is the regional scaling. Here we presented use of the parameterizations discussed earlier using both observations as well as model simulated exchanges at a regional scale. In addition to the surface observations, application of remote sensed radiometric data and the spectral indices was also linked (see Gao et al. [27]).

One of the critical issues for future research in the mesoscale deposition estimates is the propagation of uncertainty in the analysis. Despite efforts such as the National Acid Deposition Program (NADP), there is still a paucity of experimental data to validate the regional scale deposition velocity estimates under diverse atmospheric conditions. Wesley and Lesht [158] estimate an uncertainty in estimates of deposition velocity of about ±30 % even with surface homogeneity. In addition to the effect of inhomogeneity–a feature almost always encountered in

Mesoscale Atmospheric Dispersion, 2001, Ed. Z. Boybeyi, WIT Publications, Southampton, UK, Advances in Air Pollution, Vol 9, p. 424.

reality- mesoscale deposition estimates will have an uncertainty due to the interactive role of the reactive nature of depositing material. Further, most deposition and mass balance studies have been performed over continental United States and Europe and the tropics still remain largely unexplored. The vegetative feedback in the tropics is dominated by soil moisture availability [159] and hence the variations in the deposition velocity over an extended period would be of particular interest. Overall, surface wetness and temperature significantly control the bi-directional fluxes in both tropics as well as other regions of the world (see Sharkey and Singsaas [160]).

Hence, mesoscale models that do not have explicit parameterizations for surface moisture and surface temperature will have an inherently high uncertainty in estimating V_d values (see Niyogi et al. [28]). Further, the resistance parameterizations are a function of landuse type, which lead to a simplification in the mass balance procedures at a regional scale. The parameterizations are developed and often validated using observations at micrometeorological scale (few minutes, and few meters), while the estimates are applied for meso–to regional scale (Walcek et al. [161]). Wesley [24] suggests V_d estimates can be considered most appropriate for long term averages and time scales ranging over several weeks and large regions. As that, the effects of diverse surface characteristics need to be averaged to 'median' values.

Further, role of varying vegetative clusters, differences in vegetation characteristics (senescence or greening), and the chemical activity of the soil (alkalinity or acidic, see Finlayson–Pitts and Pitts [162]) is still largely unknown. Duyzer and Fowler [49] outline three additional deficiencies in the regional deposition studies. First, since deposition flux is a product of ground level concentration and deposition velocity, depending on the model vertical resolution, the average boundary layer concentration has to be converted to ground level concentration. This can be difficult for chemically active species and for topographically and physiologically variable domain [18], [163]. Second, edges of major discontinuities such as forests and water bodies act as significant sinks [140], [164]. Special routines may be thus necessary for such complex terrain with regression–based interpolations for vegetative and topographical features. Third, for mesoscale eco-physiological studies in which issues such as nutrient loading to watershed or acidic deposition to a sensitive biota are under consideration, subgrid scale processes become critical. Duyzer and Fowler [49] suggest statistical corrections for dynamical models for critical loading as a subgrid scale parameterization. In conjunction with such uncertainties, Lovblad and Erisman [165] and Erisman and Baldocchi [51], have developed interesting summary tables of the uncertainty in deposition estimates for Europe. At a regional scale, they consider deposition to be modulated by different variables such as: emission strength, wind speed, roughness length, surface wetness, orography, co-deposition, canopy resistance, dry deposition, wet deposition, cloud and fog.

Of these factors, for the entire Europe, highest uncertainty is estimated for dry deposition, in addition to factors such as surface/canopy resistance calculations, surface wetness and the role of fog and clouds that influence the deposition process. It is pertinent to recognize that most experiments undertaken for validation of the V_d modules are under fair weather conditions which may not yield range of values valid for diverse situations often possible within model grid cells. Additionally role of mechanistic models, such as the eco-physiological models described previously, at a regional scale need to be further evaluated. Also role of water films on vegetation [18], co-deposition and canopy leaching is still unresolved [51], [79]. Indeed there are large gaps in our understanding of the processes related to deposition and bi-directional fluxes, as well as translation of these effects to a regional grid structure. However, the issue is of pivotal importance for regional climate change, and socio economic policies. Thus efforts in mesoscale air pollution studies should focus on developing modules for point to area (for converting microscale observations to mesoscale grids), as well as area to point (for satellite datasets to link with tower measurements) conversions. Use of bi-directional eco-physiological models coupled with dynamical models appears to be the most promising approach in developing universal terrestrial biosphere exchange scaling relations.

Acknowledgements

This work was funded in part by the National Oceanic and Atmospheric Administration (NOAA) and the State Climate Office of North Carolina. The authors would like to acknowledge fruitful discussions with Dr. Ellen Cooter, NOAA during the course of this study. The State Climate Office

Mesoscale Atmospheric Dispersion, 2001, Ed. Z. Boybeyi, WIT Publications, Southampton, UK, Advances in Air Pollution, Vol 9, p. 424.

of North Carolina is a public service center for climate – environment interactions at the North Carolina State University.

References

[1] Niyogi D.S. & Raman S., Comparison of four different stomatal resistance schemes using FIFE data, *J. Appl. Meteor.*, **36**, pp. 903 – 917, 1997.

[2] Grantz, D., & Meinzer, F., Stomatal responses to humidity in a sugarcane field: simultaneous porometric and micrometeorological measurements', *Plant, Cell and Environ.*, **13**, pp. 27-37, 1990.

[3] Monteith J., Gas exchange in plant communities, in *Environmental Control of Plant Growth*, ed. L.T. Evans, Academic Press, New York, 1963.

[4] Hill, A., Vegetation: a sink for atmospheric pollutants, *J. Air Poll. Control Assoc.*, pp. 341 – 346, 1971.

[5] van der Hoven, I., Deposition of particles and gases, in *Meteorology and Atomic Energy*, ed. D. Slade, U. S. Atmoc Energy Commission, Office of information Services, Oak Ridge TN, USA, pp. 202 – 208, 1968.

[6] Turner, N., Rich, S., & Waggoner, P., Removal of ozone by soil, *J. Environ. Quality,* **2**, pp. 259 – 264, 1973.

[7] Turner, N., Waggoner, P., & Rich, S., Removal of ozone by soil and vegetation, *Nature,* **250**, pp. 486 – 489, 1974.

[8] Bennett, J., & Hill, A., Absorption of gaseous air pollutant by a standardized plant canopy, *J. Air Pollut. Control Assoc.,* **23**, pp. 89 – 98, 1973.

[9] Garland, J., & Penkett, S., Absorption of peroxy acetyl nitrate and ozone by natural surfaces, *Atmos. Environ.,* **10**, 1127 – 1131, 1976.

[10] Wesley, M., & Hicks, B., Some factors that affect the deposition rates of sulfur dioxide and similar gases on vegetation, *J. Air Pollut. Control. Assoc.,* **27**, pp. 1110 – 1116, 1977.

[11] Mooney, H., The carbon balance of plants, *Ann. Rev. Ecol. Syst.*, **3**, pp. 315 – 346, 1972.

[12] Pielke, R., Climate prediction as an initial value problem, *Bull. Amer. Meteor. Soc.*, **79**, pp. 2743 – 2746, 1998.

[13] Randall, D., Dazlich, D., Zhang, C., Denning, A., Sellers, P., Tucker, C., Bounoua, L., Berry, J., Collatz, G., Field, C., Los, S., Justice, C., & Fung, I., A revised land surface parameterization (SiB2) for GCMs. Part III: The greening of the Colorado State University General Circulation Model, *J. Clim.*, **9**, pp. 738 – 763, 1996.

[14] Foley, J., Prentice, C., Ramankutty, N., Levis, S., Pollard, D., Stich, S., & Haxeltine, A., 1996, An integrated biosphere model of land surface processes, terrestrial carbon balance, and vegetation dynamics, *Glob. Biogeochem. Cyc.*, **10**, pp.603 – 628, 1996.

[15] Cox, P., Betts, R., Bunton, C., Essery, R., Rowntree, P., & Smith, J., The impact of new land surface physics on the GCM simulation on climate and climate sensitivity, *Clim. Dynamics*, **15**, pp. 183 – 203, 1999.

[16] Holt T., & Raman S., A review and comparative evaluation of multi-level boundary layer parameterizations for first order and turbulent kinetic energy closure schemes, *Rev. Geophys.*, **26**, pp. 761-780, 1988.

[17] Stull, R., An introduction to boundary layer meteorology, Kluwer Academic Publishers, Dordrecht, pp. 666, 1988.

[18] Arey, J., Winer A., Atkinson, R., Aschman, S., Long, W., Marrison, C., & Olszyk, D., Terpenes emitted from agricultural species found in California's central valley, *J. Geophys. Res.*, **96**, pp. 9329 – 9336, 1991.

[19] Chameides, W., Lindsay, R., Richardson, J., & Kiang, C., The role of biogenic hydrocarbons in urban photochemical smog: Atlanta as a case study, *Science*, **241**, pp. 1473 – 1475, 1990.

[20] Monson, R., & Fall, R., Isoprene emissions from Aspen leaves. The influence of environment and relationship to photosynthesis and photorespiration, *Plant Physiol.*, **90**, pp. 267 – 274, 1989.

[21] Langford, A., & Fehsenfeld, F., Natural vegetation as a source or sink for atmospheric ammonia: a case study, *Science*, **255**, 581 – 583, 1992.

[22] Guenther, A., Zimmerman, P., & Harley, P., Isoprene and Monoterpene emission rate variability: Model evaluations and sensitivity analyses, *J. Geophys. Res.*, **98**, pp. 12609 – 12617, 1993.

[23] Fitzgerald, W., Is mercury increasing in the atmosphere? The need for an atmospheric mercury network, *Water, Air, and Soil Pollution*, **80**, pp. 245 – 254, 1995.

[24] Wesely, M., Parameterization of surface resistance to gaseous dry deposition in regional scale numerical models, *Atmos. Environ.*, **23**, pp. 1293 – 1304, 1989.

[25] Fowler, D., & Unsworth, M., Turbulent transfer of sulfur dioxide to a wheat canopy, *Q. J. Roy. Meteor. Soc.*, **105**, pp. 767 – 783, 1979.

[26] Fuentes, J., & Gillespie, T., A gas exchange system to study the effects of leaf surface wetness on deposition of ozone, *Atmos. Environ.*, **26**, pp. 1165 – 1173, 1991.

[27] Gao., W., Wesley, M., Cook, D., Hart, R., Air – surface exchange of H20, CO2, and O3 at a tall grass prairie in relation to remotely sensed vegetation indices, *J. Geophys. Res.*, **97**, pp. 18663 – 18671, 1992.

[28] Niyogi, D., Raman, S., & Alapaty, K., A dry deposition model that includes vegetation - atmosphere interactions through photosynthesis / gas Assimilation, *Atmos. Environ.,* in review, 1999.

[29] Xu, X., Yang, X., Miller D., Helble, J., & Carley, R., Formulation of bi-directional atmosphere – surface exchanges of elemental mercury, *Atmos. Environ.*, **33**, pp. 4345 – 4355, 1999.

[30] Businger, J., Evaluation of the accuracy with which dry deposition can be measured with current micrometeorological techniques, *J. Appl. Meteor.*, **25**, pp. 1100 – 1124, 1986.

[31] Droppo, J., Concurrent measurements of ozone dry deposition using eddy correlation and flux profile methods, *J. Geophys. Res.*, **90**, pp. 2111 – 2118, 1985.

[32] Beljaars, A., & Holstlag, A., Flux parameterization over land surfaces for atmospheric models, *J. Appl. Meteor.*, **30**, pp. 327 – 341, 1991.

[33] Monin, A.S., & A.M. Yaglom, *Statistical Fluid Mechanics. Vol. I*, MIT Press, Cambridge, pp. 468-504, 1971.

[34] Baldocchi, D., Hicks, B., & Camara, P., A canopy stomatal resistance model for gaseous deposition to vegetated surfaces, *Atmos. Environ.*, **21**, pp. 91 – 101, 1987.

[35] Baldocchi, D. & Meyers, T., On using eco-physiological, micrometeorological, and biogeochemical theory to evaluate carbon dioxide, water vapor, and trace gas fluxes over vegetation: Synthesis and application, *Agric. Forest Meteorol.*, **90**, pp. 1 – 25, 1995.

[36] Kustas, W., Estimated values of evapotranpiration with one and to layer model of heat transfer over partial canopy cover, *J. ppl. Meteor.*, **29**, pp. 704 – 715, 1990.

[37] Owen, P., & Thompson, W., Heat transfer across rough surfaces, *J. Fluid Mech.*, **15**, pp. 321 – 334, 1963.

[38] Kramm, G., Beier, N., Foken, T., Muller, H., Schroder, P., & Seiler, W., A SVAT for NO, NO2, and O3 - Model description and test results, *Meteor. Atmos. Physics,* **61**, pp. 89 – 106, 1996.

[39] Parlange, Y., Waggoner, P., & Heichel, G., Boundary layer resistance and temperature distribution on still and flapping leaves. I. Theory and Laboratory experiments, *Plant Physiol.*, **48**, pp. 437 – 442, 1971.

[40] Leuning, R., Neumann, H., & Thurtell, G., Ozone uptake by corn: a general approach, *Agric. Meteorol.*, **20**, pp. 115 – 136, 1979.

[41] Schlichting, H., *Boundary Layer Theory*, Translated by J. Kestin, McGraw-Hill, New York, pp. 647, 1960.

[42] Brutsaert, W., *Evaporation into the Atmosphere*, D. Reidel Publishing Company, Dordrecht, 1982.

[43] Draxler, R., & Hess, G., *Description of the HySplit-4 modeling system*, NOAA Tech. Mem. ERL/ ARL –224, 1997. [Available from http://www.arl.noaa.gov/READY]

[44] Draxler, R., & Hess, G., An Overview of the Hysplit_4 Modeling System for Trajectories, Dispersion, and Deposition, *Aust. Met. Mag.*, **47**, pp. 295-308, 1998.

[45] Padro, J., Observed characteristics of the dry deposition velocity of O_3 and SO_2 above a wet deciduous forest, *Sci. Tot. Environ.*, **146/147**, pp. 395 – 400, 1994.

[46] Chang, J., Brost, R., Isaksen, I., Madronich, S., Middleton, P., Stockwell, W., & Walcek, W., A three dimensional Eulerian acid deposition model: physical concepts and formulation, *J. Geophys. Res.*, **92**, pp. 14681 – 14700, 1987.

[47] Sehmel, G., Particle and gas dry deposition: a review, *Atmos. Environ.*, **14**, pp. 983 – 1012, 1980.

[48] Voldner, E., Barrie, L., & Sirois, A., A literature review of dry deposition of oxides of sulphur and nitrogen with emphasis on long range transport modeling in North America, *Atmos. Environ.*, **20**, pp. 2101 – 2123, 1986.

[49] Duyzer, J., & Fowler, D., Modeling land atmosphere exchange of gaseous oxides of nitrogen in Europe, *Tellus*, **46B**, pp. 353 – 372, 1994.

[50] Erisman, J., Beier, C., Draaijers, G., & Lindberg, S., Review of deposition monitoring methods, *Tellus*, **46**, pp. 79 – 93, 1994.

[51] Erisman, J., & Baldocchi, D., Modeling dry deposition of SO_2, *Tellus*, **46B**, pp. 159 – 171, 1994.

[52] Arya, S., *Introduction to Micrometeorology*, Academic Press, San Diego, pp. 307, 1988.

[53] Arya, S., *Air pollution meteorology and dispersion*, Oxford University Press, New York, pp. 310, 1999.

[54] Pleim, J.E., Finkelstein, P., Ellestad, T.G., A technique for estimating dry deposition velocities based on similarity with latent heat flux, *Atmos. Environ*., **33**, pp. 2257 – 2265, 1999.

[55] Brook, J., Di-Giovanni, F., Meyers, T., Estimation of dry deposition velocity using inferential models and site-specific meteorology-Uncertainty due to siting of meteorological towers. *Atmos. Environ.,* **31**, pp. 3911 – 3920, 1997.

[56] Niyogi, D., Raman, S., & Alapaty K., Uncertainty in specification of surface characteristics, Part 2: Hierarchy of interaction explicit statistical analysis, *Boundary-Layer Meteorol.*, **91**, pp. 341 – 366, 1999.

[57] Travis, C., & Hattemer – Frey, H., Uptake of organics by aerial plant parts: A call for research, *Chemosphere*, **17**, pp. 277 – 283, 1988.

[58] Garland, J., The dry deposition of sulfur dioxide to land and water surfaces, *Proc. R. Soc. Lond.,* **12**, pp. 245 - 268, 1977.

[59] Lynn, B., & Carlson, T., A stomatal resistance model illustrating plant vs. external control of transpiration', *Agric. For. Meteorol.,* **52**, pp.5-43, 1990.

[60] Niyogi, D., Raman, S., & Alapaty, K., Comparison of four different stomatal resistance schemes using FIFE observations, Part 2: Analysis of terrestrial biospheric-atmospheric interactions, *J. Appl. Meteorol.,* **37**, pp. 1301 – 1320, 1998.

[61] Niyogi D., Alapaty K., Raman S. (1999a) An advanced carbon assimilation B surface evapotranspiration scheme for mesoscale models, MM5 Workshop on Land Surface Modeling and its Application to Mesoscale Models, 24 - 25 June 1999, Boulder CO.

[62] Niyogi, D., Alapaty, K., & Raman, S., A gas exchange / assimilation surface evapotranspiration model (GEM) for mesoscale applications, *J. Appl. Meteorol.,* in review, 1999.

[63] Cowan, I., Regulation of water use in relation to carbon gain in higher plants', in *Encylopedia of Plant Physiology*, *New Series, Vol. 12B, Physiological Plant Ecology II,* eds. Lange O., Nobel P.,

Osmond C., & Zeigler H., Springer Verlag, Berlin, pp.589-615, 1982.

[64] Jarvis, P., The interpretation of leaf water potential and stomatal conductance found in canopies in field, *Phil. Trans. R. Soc. Lond. B.*, **273**, 593 – 610, 1976.

[65] Niyogi, D., Raman, S., Alapaty, K., & Han J., A Dynamic Statistical Experiment for Atmospheric Interactions, *Environ. Model. Assess. (A)*, **2,** pp. 307 – 322, 1997.

[66] Avissar, R., Avissar, P., Mahrer, Y., & Bravdo, B., A model to simulate response of plant stomata to environmental conditions', *Agric. For. Meteorol.*, **34**, pp. 21-29, 1985.

[67] Schulze, E., Kelliher, F., Korner, C., Lloyd, J., & Leuning R., Relationships among maximum stomatal conductance, ecosystem surface conductance, carbon assimilation rate, and plant nitrogen nutrition: A global ecology scaling exercise', *Ann. Rev. Ecol. Syst.*, **25**, pp. 629-660, 1994.

[68] Kelliher, F., Leuning, R., Raupach, M., Schulze, E., Maximum conductances for evaporation from global vegetation types, *Agric. For. Meteor.*, **73**, pp. 1 – 16, 1995.

[69] Alapaty, K., Pleim, J., Raman, S., Niyogi, D. S., & Byun, D., Simulation of Atmospheric Boundary Layer Processes using Local - and Nonlocal-Closure Schemes *J. Appl. Meteorol.*, **36**, pp. 214 – 233, 1997.

[70] Wetzel P., & Chang J., Evapotranspiration from non-uniform surface: A first approach for short-term numerical weather prediction, *Mon. Wea. Rev.*, **116**, pp. 600-621, 1988.

[71] Dickinson, R., Henderson-Sellers, A., Kennedy, P., & Wilson M., *Biosphere-atmosphere transfer scheme (BATS) for the NCAR community climate model*, NCAR / TN - 275 + STR, 1986. [Available from the National Center for Atmospheric Research, Boulder, CO].

[72] Noilhan, J., & Planton, S., A simple parameterization of land surface processes for meteorological models', *Mon. Wea. Rev.*, **117**, pp. 536-549, 1989.

[73] Clapp, R., & Hornberger, G., Empirical equations for some soil hydraulic properties, *Wat. Resources Res.*, **14**, pp. 601 – 604, 1978.

[74] Cosby, B., Hornberger, G., Clapp, R., Ginn, T., A statistical exploration of the relationships of soil moisture characteristics to the physical properties of soil, *Wat. Resources Res.,* **20**, 682 – 690, 1984.

[75] Walmsley, P., & Wesely, M., Modification of coded parametrizations of surface resistances to gaseous dry deposition, *Atmos. Environ*., **30**, pp. 1181 – 1196, 1996.

[76] Sutton, M., Pitcairn, C., & Fowler, D., The exchange of ammonia between the atmosphere and the plant communities, *Advances Ecol. Res.*, **24**, pp 301 – 393, 1993.

[77] Underwood, B., Dry deposition to a uniform canopy: evaluation of a first – order- closure mathematical model, *Atmos. Environ.*, **21**, pp. 1573 – 1585, 1987.

[78] Horst, T., A surface depletion model for deposition from a Gaussian plume, *Atmos. Environ.,* **11**, pp. 41 – 46, 1977.

[79] Sutton, M., Burkhardt, J., Guerin, D., Nemitz, E., & Fowler, D., Development of resistance models to describe measurements of bi-directional ammonia surface - atmosphere exchange, *Atmos. Environ.*, **32**, pp. 473 – 480, 1998.

[80] Farquhar, G., Firth, P., Wetselaar, R., & Weir, B., On the gaseous exchange of ammonia between leaves and the environment: determination of the ammonia compensation point, *Plant Physiol.*, **66**, pp. 710 – 714, 1980.

[81] Farquhar, G., Wetselaar, R., & Weir, B., Gaseous nitrogen losses from plants, in *Gaseous Loss of Nitrogen from Plant – Soil Systems*, ed. J. R. Freeny, & J. R. Simpson, Nijhoff / Dr. W. Junk Publishers, The Hague, pp. 159 – 180, 1983.

[82] Hanson, P., Lindberg, S., Tabberer, T., Owens, J., & Kim, K., Foliar exchange of mercury vapor: evidence for a compensation point, *Water, Air, Pollution*, **80**, pp. 373 – 382, 1995.

[83] Mahfouf, J., Analysis of soil moisture from near-surface parameters. A feasibility study, *J. Appl. Meteor*., **30**, pp. 461 – 467, 1991.

[84] Deardorff, J., Efficient prediction of ground surface temperature and moisture with inclusion of a layer of vegetation, *J. Geophy.Res.*, **20**, pp. 1889-1903, 1978.

[85] Xue Y., Sellers P., Kinter J., & Shukla J., A simplified biosphere model for climate studies', *J. Clim*., **4**, pp. 345-364, 1991.

[86] Acs, F., A coupled Soil-Vegetation Scheme: Description, Parameters, Validation and Sensitivity Studies, *J. Appl. Meteor.*, **33**, pp 268-284, 1994.

[87] Monteith, J., & Unsworth, M., *Principles of Environmental Physics*, Edward Arnold, London, pp. 291, 1990.

[88] Raupach, M., Vegetation-atmosphere interaction in homogeneous and heterogeneous terrain: some implications of mixed-layer dynamics', *Vegetatio*, **91**, 105-120, 1991.

[89] Carpi, A., & Lindberg, S., Application of a Teflon dynamic flux chamber for quantifying soil mercury flux: tests and results over background soil, *Atmos. Environ.*, **32**, pp. 873 – 882, 1998.

[90] Harley, P., Guenther., A., & Zimmerman, P., Environmental controls over isoprene emission in deciduous oak canopies, *Tree Physiol.*, **17**, pp. 705 – 714, 1997.

[91] Lemon, E., & van Houtte, R., Ammonia exchange at the land surface, *Agron. J*., **72**, pp. 876 – 883, 1980.

[92] Fowler, D., Flechard, C., Sutton, M., & Storeton-West, R., Long term measurements of the land - atmosphere exchange of ammonia over moorland, *Atmos. Eviron.*, **32**, pp. 453 – 459, 1998.

Mesoscale Atmospheric Dispersion, 2001, Ed. Z. Boybeyi, WIT Publications, Southampton, UK, Advances in Air Pollution, Vol 9, p. 424.

[93] Schjoerring, J., Husted, S., & Mattsson, M., Physiological parameters controlling plant – atmosphere ammonia exchange, *Atmos. Environ.*, **32**, pp. 491 – 498, 1998.

[94] Monson, R., Lerdau, M., Sharkey, T., Schimel, D., & Fall, R., Biological aspects of constructing VOC emission inventories, *Atmos. Environ.*, **29**, pp. 2989 – 3002, 1995.

[95] Nikolov, N., Massman, W., Schoettle, A., Coupling biochemical and biophysical processes at the leaf level: an equilibrium photosynthesis model for leaves of C3 plants', *Ecol. Modeling*, **80**, pp. 205-235, 1995.

[96] Sutton, M., Schjoerring, J., & Wyers, P., Plant – atmosphere exchange of ammonia, *Phil. Trans. Roy. Soc. London,* **351**, pp. 261 – 278, 1995.

[97] Meyers, T., & Paw U., K., Modeling the plant canopy micrometeorology with higher-order closure principles, *Agri. For. Meteor.*, **41**, pp. 143-163, 1987.

[98] Meyers, T., & Baldocchi, D., A comparison of models for deriving dry deposition fluxes of O_3 and SO_2 to forest canopy, *Tellus*, **40B**, pp. 270 – 284, 1988.

[99] Sutton, M., Asman, W., & Schjorring, J., Dry deposition of reduced nitrogen, *Tellus*, **46B**, pp. 255 – 273, 1994.

[100] Asman, W., Factors influencing local dry deposition of gases with special reference to ammonia, *Atmos. Environ.*, **32**, 41 – 421, 1998.

[101] Rondon, A., & Granat, L., Studies on the dry deposition of NO_2 to coniferous species at low NO_2 concentrations, *Tellus*, **46B**, pp. 339 – 352, 1994.

[102] Niyogi, D., & Raman, S., Dynamical Coupling of Heterogeneous fluid media for an environmental interface, Proc. 1st Intrnl. Conf. Fluid Mech. Fluid Power, Dec 15 - 17, Delhi, IIT Delhi, New Delhi, pp. 107-110, 1998.

[103] Niyogi D., Alapaty K., & Raman S., Developing multi-media couplings to link ambient meteorological information with depositing surface environment, Workshop on Atmospheric

Nitrogen Compounds: Emissions Transport, Transformation, Deposition, and Assessment, June 7 B 9 1999, Chapel Hill, NC, 1999.

[104] Elssworth, D.,Water relations and gas exchange of *Acer saccharum* seedlings in contrasting natural light and water regime, *Tree Physiol.*, **10**, pp. 1-20, 1992.

[105] Wong, S., Cowan, I., & Farquhar G., Stomatal conductance correlates with photosynthetic capacity, *Nature*, **282**, pp. 424 – 426, 1979.

[106] Farquhar, G., von Caemmerer, S., & Berry, J., A biochemical model of photosynthetic CO2 assimilation in leaves of C3 species', *Planta*, **149**, pp. 78-90, 1980.

[107] Farquhar, G., & Sharkey, T., 'Stomatal Conductance and Photosynthesis', *Ann. Rev. Plant Physiol.*, **33**, 00. 317-345, 1982.

[108] Ball, J., Calculations related to gas-exchange. In *Stomatal Function*, ed. E. Zeiger, G.D. Farquhar, &I.R. Cowan, Stanford University Press, Stanford, pp. 445 – 476, 1987.

[109] Ball J., Woodrow I., & Berry J., A model predicting stomatal conductance and its contribution to the control of photosynthesis under different environmental conditions, In *Progress in Photosynthetic Research*, ed. J. Biggins Vol IV, Martinus Nijhoff Publishers, Dordrecht, 1987.

[110] Aphalo, P., & Jarvis, P., Do stomata respond to relative humidity?, *lant, Cell and Environ.*, **14**, pp. 127-132, 1991.

[111] Mott, K., & Parkhurst, D., Stomatal response to humidity in air and elox, *Plant, Cell, Environ.*, **14**, pp. 509 – 515, 1991.

[112] Monteith, J., A reinterpretation of stomatal responses to humidity', *Plant, Cell Environ.*, **18**, 357 – 364, 1995.

[113] Monteith, J., Accomodation between transpiring vegetation and the convective boundary layer', *J. Hydrol.*, 166, 251- 254, 1995.

[114] Mooney, H., Vitousek, P., Matson, P., Exchange of materials between terrestrial ecosystems and the atmosphere, *Science*, **238**, pp. 926 – 932, 1987.

[115] Hosker, R., & Lindberg, S., Review: Atmospheric deposition and plant assimilation of gases and particles, *Atmos. Environ.*, **16**, 889 – 910, 1982.

[116] Collatz, G., Ball, J., Grivet, C., & Berry, J., Physiological and environmental regulation of stomatal conductance, photosynthesis and transpiration: a model that includes a laminar boundary layer', *Agric. For. Meteorol.*, **54**, pp. 107-136, 1991.

[117] Collatz, G., Ribas-Carbo, M., & Berry, J., Coupled photosynthesis-stomatal conductance model for leaves of C4 plants, *Aust. J. Plant Physiol.*, **19**, pp. 519-538, 1992.

[118] Sellers, P., Berry, J., Collatz, G., Field, C., & Hall, F., Canopy reflectance, photosynthesis and transpiration, III. A reanalysis using enzyme – kinetics – electron transport models of leaf physiology, *Remote Sens. Environ.*, **42**, pp. 187 – 216, 1992.

[119] Calvet, J., Noilhan, J., Roujean, J., Bessemoulin, P., Cabelguenne, M., Olioso, A., & Wigneron, J., An interactive vegetation SVAT model tested against data from six contrasting sites, *Agric. For. Meteor.*, **92**, pp. 73 – 95, 1998.

[120] Goudriaan, J., van Laar, H., van Keulen, H., & Louwerse, W., Photosynthesis, CO_2, and plant production, *Wheat growing and modeling, NATO ASI Series, Series A, Vol 86*, ed. W. Day, & R. Atkin, Plenum Press, New York, pp. 107 – 122, 1985.

[121] Kim J., & Verma S., Modeling canopy photosynthesis: scaling up from a leaf to canopy in a temperate grassland ecosystem, *Agri. For. Meteorol.*, **57**, pp. 187 – 208, 1991.

[122] van Heemst, Potential crop production, in Modeling of agricultural production: weather, soil, and crops, ed. H. van Keulen & J. Wolf, Simulation Monograph, Pudoc, Wageningen, 1986.

[123] Jacobs, C., van den Hurk, B., de Bruin, H., Stomatal behavior and photosynthetic rate of unstressed grapevines in semi-arid conditions, *Agric. For. Meteor.*, **80**, pp. 111 – 134, 1996.

[124] Jacobs, C., Direct impact of atmospheric CO2 enrichment on regional transpiration', Ph.D. thesis, Wageningen Agricultural University, The Netherlands, pp. 1- 179, 1994. [Available from the Department of Meteorology, Wageningen Agricultural University, Duivendaal 2, 6701 AP Wageningen, The Netherlands].

[125] Sellers, P., Randall, D., Collatz, J., Berry, J., Field, C., Dazlich, D., Zhang, C., Collelo, G., & Bounous A., A revised land surface parameterization (SiB2) for atmospheric GCMs: Model formulation, *J. Clim.*, **9**, pp. 676-705, 1996.

[126] Sellers P., Los, S., Compton, T., Justice, C., Dazlich, D., Collatz J., Randall, D., A revised land surface parameterization (SiB2) for atmospheric GCMs. Part II: The generation of global fields of terrestrial biophysical parameters from satellite data, *J. Clim.*, **9**, pp. 706-736, 1996.

[127] Su, H.B., Paw U, K.T., & Shaw, R., Development of a coupled leaf and canopy model for the simulation of plant-atmosphere interaction, *J. Appl. Meteor.*, **35**, pp. 734-748, 1996.

[128] Jones, H., *Plants and Microclimate, A quantitative approach to environmental plant physiology*, Cambridge University Press, Cambridge U.K. and New York USA, pp. 428, 1992.

[129] Baldocchi, D., A Lagrangian Random-Walk model for simulating water vapor, CO2, and sensible heat flux densities and scalar profiles over and within a soybean canopy', *Bound. -Layer Meteorol.*, **61**, pp. 113-144, 1992.

[130] Baldocchi, D., A comparative study of mass and energy exchange over a closed C3 (Wheat) and an open C4 (Corn) canopy: The partitioning of available energy into latent and sensible heat exchange', *Agric. For. Meteorol.*, **67**, pp. 191-220, 1994.

[131] Choudhury, B., & Montieth, J., Implications of stomatal response to saturation deficit for the heat balance of vegetation, *Agric. For. Meteorol.*, **36**, pp. 215-225, 1986.

Mesoscale Atmospheric Dispersion, 2001, Ed. Z. Boybeyi, WIT Publications, Southampton, UK, Advances in Air Pollution, Vol 9, p. 424.

[132] Dougherty, R., Bradford, J., Coyne, P., & Sims, P., Applying an empirical model of stomatal conductance to three C-4 grasses, *Agric. For. Meteorol.*, **67**, pp. 269-290, 1994.

[133] Sandnes H., & Styve H. Calculated budgets for airborne acidifying component in Europe, 1985, 1987, 1988, 1989, 1990, and 1991. EMEP Report 1/92. Norwegian Meteor. Inst. Oslo, Norway. (ISSN 0332-9879), 1992.

[134] van Aalst, R., Dry deposition of NO_x, in *Air Pollution by Nitrogen Oxides*, ed. T. Schneider, & L. Grant, Elsevier, Amsterdam, pp. 263 – 270, 1982.

[135] Hanson, P., & Lindberg, S., Dry deposition of reactive nitrogen compounds: A review of leaf, canopy and non-foliar measurements, *Atmos. Environ.*, **25A**, pp. 1615 – 1634, 1991.

[136] Hanson, P., Rott, K., Taylor, G., Gunderson, C., Lindberg, S., & Ross – Todd, B., NO2 deposition to elements representative of a forest landscape, *Atmos. Environ.*, **23**, pp. 1783 – 1794, 1989.

[137] Judeikis, H., & Wren, A., Laboratory measurements of NO and NO2 deposition onto soil and cement surfaces, *Atmos. Environ.*, **12**, pp. 2315 – 2319, 1978.

[138] Niyogi, D., Raman, S., Prabhu, A., Kumar, A., Joshi, S., Direct estimation of stomatal resistance for meteorological applications, *Geophys. Res. Lett.*, **24**, pp. 1771 – 1774, 1997.

[139] Erisman, J., Bleeker, A., & Jaarsveld, H., Atmospheric deposition of ammonia to semi-natural vegetation in the Netherlands - Methods for mapping and evaluation, *Atmos. Environ.*, **32**, pp 481 – 489, 1998.

[140] Rondon, A., Johansson, C., & Granat, L., Dry deposition of nitrogen dioxide and ozone to coniferous forests, *J. Geophys. Res.*, **98D**, 5159 – 5172, 1993.

[141] Cohen Y., & Ryan P., Mass transfer across wind-sheared interfaces, *Int. Comm. Heat Mass Transfer*, **12**, pp. 139 – 148, 1985.

[142] Pasquill, F., & Smith, F., Atmospheric Diffusion; the dispersion of windborne material from industrial and other sources, Ellis Horwood, Chichester, UK, pp. 297, 1983.

[143] Singles, R., Sutton, M., Weston, K., A multi-layer model to describe the atmospheric transport and deposition of ammonia in Great Britain, *Atmos. Environ.*, **32**, 393 – 399, 1998.

[144] Taconet, O., Bernard, R., & Vidal – Madjar, D., Evapotranspiration over an agriculture region using a surface flux / temperature model based on NOAA – AVHRR data, *J. Clim. Appl. Meteor.*, **25**, pp. 284 – 307, 1986.

[145] Nemani, R., & Running, S., Testing a theoretical climate – soil- leaf area hydrological equilibrium of forests using satellite data and ecosystem simulation, *Agric. For. Meteor.*, **44**, pp. 245 – 260, 1989.

[146] Asrar, G., Fuchs, m., Kanemasu, E., & Hatfield, J., Estimating absorbed photosynthetic radiation and leaf area index from spectral reflectance in wheat, *Agron. J.*, **76**, pp. 300 – 306, 1984.

[147] Tarpley, J., Schneider, S., & Money, R., Global vegetation indices from the NOAA-7 meteorological satellite, *J. Clim. Appl. Meteor.*, **23**, 491 – 494, 1984.

[148] Tucker, C., Vanpraet, C., Sharman, M., & van Itersum, G., Satellite remote sensing of total herbaceous biomass production in the Senegalese Sahel: 1980 – 1984, *Remote Sens. Environ.*, **17**, pp. 233 – 249, 1985.

[149] Nemani, R., & Running, S., Estimation of regional surface resistance to evapotranspiration from NDVI and Thermal –IR AVHRR data, *J. Appl. Meteor.*, **28**, pp. 276 – 284, 1989.

[150] Cihlar, J., St. Laurent, L., Dyer, J., Relation between the normalized difference vegetation index and ecological variables, *Remote Sens. Environ.*, **8**, pp. 279 – 298, 1991.

[151] Seevers, P., & Ottmann, R., Evapotranspiration estimation using a normalized difference vegetation index transformation of satellite data, *Hydrol. Sciences*, **39**, pp. 333 – 345, 1994.

Mesoscale Atmospheric Dispersion, 2001, Ed. Z. Boybeyi, WIT Publications, Southampton, UK, Advances in Air Pollution, Vol 9, p. 424.

[152] Szilagyi, J., Rundquist, D., Gosselin, D., & Parlange, M., NDVI relationship to monthly evaporation, *Geophys. Res. Let.*, **25**, pp. 1753 – 1756, 1998.

[153] Sellers, P., Canopy reflectance, photosynthesis and transpiration, *Int. J. Remote Sens.*, **6**, pp. 1335 – 1372, 1985.

[154] Sellers, P., Canopy reflectance, photosynthesis and transpiration Part II: The role of biophysics in the linearity of their interdependence, *Remote Sens. Environ.*, **21**, pp. 143 – 183, 1987.

[155] Charles – Edwards, D., & Ludwig, L., A model for leaf photosynthesis by C3 plant species, *Ann. Bot.*, **38**, pp. 921 – 934, 1974.

[156] Goudriaan, J., The bare bones of leaf-angle distribution in radiation models for canopy photosynthesis and energy exchange', *Agric. For. Meteorol.*, **43**, pp. 155-169, 1988.

[157] Asrar, G., *Theory and Applications of Optical Remote Sensing*, Wiley Interscience, New York, pp. 734, 1990.

[158] Wesley, M., & Lesht, B., *Comparison of the RADM dry deposition module with site – specific routines for inferring dry deposition*, EPA/600 / S4-88/027, U.S. Environmental Protection Agency (available as PB88-238191/AS from NTIS, Springfield VA), 1988.

[159] Raman, S., Niyogi, D., Prabhu, A., Ameenullah S., Nagaraj, S., Jayyanna, K., Udai Kumar, VEBEX: A Vegetation and Energy Balance Experiment for the Tropics, *Proc. Ind. Acad. Sci. (Earth and Planetary Sciences)*, **107**, pp. 97 – 105, 1997.

[160] Sharkey, T., & Singsaas, E., Why plants emit isoprene?, *Nature*, **374**, pp. 769, 1995.

[161] Walcek, C., Brost, R., Chang, J., & Wesley, M., SO_2, sulfate, and HNO_3 deposition velocities computed using regional landuse and meteorological data, *Atmos. Environ.*, **21**, pp. 1759 – 1763, 1986.

[162] Finlayson – Pitts, B., & Pitts, J., *Atmospheric Chemistry: Fundamentals and Experimental Techniques*, John Wiley and Sons, New York, pp. 1098, 1986.

Mesoscale Atmospheric Dispersion, 2001, Ed. Z. Boybeyi, WIT Publications, Southampton, UK, Advances in Air Pollution, Vol 9, p. 424.

[163] Finnigan, J., & Raupach, M., Transfer processes in plant canopies in relation to stomatal characteristics, in *Stomatal Function*, ed. E. Zeiger, G. Farquhar, I. Cowan,. Stanford Univ Press, Stanford, CA, pp. 385-429, 1987.

[164] Baldocchi, D., & Rao, K.S., Intra-field variability of scalar flux densities across a transition between a desert and an irrigated potato field', *Bound. -Layer Meteorol.*, **76**, pp.109-121, 1995.

[165] Lovblad, G., & Erisman, J., Deposition of nitrogen in Europe, *Critical loads for Nitrogen,* Eds. P. Grennfelt, & E. Thornelof, Lokeberg, 6 – 10 April 1992, Sweden, Report No. Nord 1992:41, Nordic Council of Ministers, Copenhagen, Denmark, pp. 239 – 286, 1992.